Fabrication of Protein Nanoarrays via Colloidal Lithography

by

Huiyan Li
B.Eng, Harbin Institute of Technology, 2006

A Thesis Submitted in Partial Fulfillment
of the Requirements for the Degree of

MASTER OF APPLIED SCIENCE

in the Department of Electrical and Computer Engineering

Fabrication of Protein Nanoarrays via Colloidal Lithography

by

Huiyan Li
B.Eng, Harbin Institute of Technology, 2006

Supervisory Committee

Dr. Chris Papadopoulos, (Department of Electrical and Computer Engineering)
Supervisor

Dr. Poman P. M. So, (Department of Electrical and Computer Engineering)
Departmental Member

Dr. Alexandre G. Brolo, (Department of Chemistry)
Outside Member

Abstract

Supervisory Committee
Dr. Chris Papadopoulos, (Department of Electrical and Computer Engineering)
Supervisor
Dr. Poman P. M. So, (Department of Electrical and Computer Engineering)
Departmental Member
Dr. Alexandre G. Brolo, (Department of Chemistry)
Outside Member

Nanoscale protein arrays have shown promise for biological and biomedical applications. Compared to traditional protein arrays, nanoarrays have the potential for higher throughput, better sensitivity, and require less sample volumes. In this thesis, protein nanoarrays were fabricated using a simple and inexpensive "natural lithography" approach. This method allows the fabrication of large-area ordered nanoparticle arrays consisting of metallic dots with tunable diameters down to 10 nm or less.

The nanoparticle arrays are formed by depositing metal through the openings of colloidal monolayer polystyrene sphere masks. After removing the masks, nanoarrays remain and are exposed to further processing. COOH-terminated self-assembled monolayers (SAM) and N-hydroxysuccinimide (NHS) chemistry is used for surface functionalization. These surface modifications covalently attach proteins onto the nanoparticles. A single monolayer of immunoglobulin G (IgG) molecules is successfully attached on the functionalized surfaces and the bioactivity of the protein arrays is tested by attaching anti-IgG molecules, as a standard immunological assay.

Results of fabrication trials and efforts to control nanoparticle size, spacing, and surface adhesion are described. Atomic force microscopy (AFM) and scanning electron microscopy (SEM) images of hexagonal gold nanoarrays consisting of approximately 150 nm particles and 3.5×10^{8} -1.5×10^{9} per cm^2 array density is shown, depending on the size of colloidal spheres. An increased height of approximately 6 nm characterized via scanning probe methods shows the attachment of a single monolayer of protein molecules to the nanoparticles. This was confirmed with SEM. A similar height increase was detected via AFM showing the attachment of anti-IgG molecules onto IgG functionalized particles. Potential applications of the protein nanoarrays and future work are discussed.

Table of Contents

List of Tables

List of Figures

Acknowledgments

I would like to express my gratitude to all those who gave me the possibility to complete this thesis. I want to thank the Department of Electrical and Computer Engineering for giving me permission to commence my degree and to do the necessary research work.

I am deeply indebted to my supervisor Prof. Dr. C. Papadopoulos whose help, stimulating suggestions, and encouragement helped me in all the time of research and writing of this thesis.

Ph.D. candidate Mr. Badr Omrane and former Master's student Ms. Susan Winnitoy in our group supported me in my research work. I want to thank them for all their help, support, interest and valuable hints.

1. Introduction

1.1 Nanotechnology

1.1.1 Definition

According to the U.S. National Nanotechnology Initiative (NNI)'s definition, nanoscience "involves research to discover new behaviors and properties of materials with dimensions at the nanoscale, which ranges roughly from 1 to 100 nanometers [1]. Nanotechnology is the way discoveries made at the nanoscale are put to work." Nanotechnology has a wide range of applications – nanoscale materials find use in electronics, photonics, biomedicine, cosmetics, energy, etc. One reason for this wide reaching coverage is that nanoscale materials differ in many ways from large-scale or bulk materials, as described below.

1.1.2 Background and Development of Nanotechnology

Although humans have implicitly employed nanotechnology for thousands of years, the concept of nanotechnology was not directly proposed until 1959, when the physicist Richard Feynman gave a talk entitled "There is Plenty of Room at the Bottom" at an American Physical Society meeting at Caltech. In this talk he described a possibility of manipulating individual atoms and molecules using precise tools, and the scaling issues

that would change physical properties were mentioned [2]. Feynman's pioneering vision went largely unnoticed for decades.

In 1974, the term "nanotechnology" was defined in a paper by Norio Taniguchi [3]. The invention of Scanning Tunneling Microscopy (STM) and Atomic Force Microscopy (AFM) in 1981 and 1986, respectively, provided powerful tools for nanoscale research [4]. Carbon-based nanostructures or fullerenes were synthesized and purified in the early 1990s, and hundreds of researchers in government and industrial laboratories began to characterize and functionalize them. By this time, nanotechnology was being recognized as a promising area to a wide range of sciences and technologies throughout the world. Described as the next industrial revolution by Peterson [5], the development of nanotechnology has now become an important endeavor in many nations. In the year 2005, the government nanotechnology expenditures in the USA, Europe, Japan, and other countries reached $1081 million, $1050 million, $950 million, and $1000 million, respectively [6]. The total global expenditure was 945% of that in the year 1997. It is estimated that by the year 2015, $1 trillion worth of products worldwide will employ nanotechnology in key functional components [6].

1.1.3 Properties of Nanomaterials

Two-dimensional (2D) structures are nanomaterials confined in one spatial dimension. For example, semiconductor quantum wells are well known 2D materials. Similarly, one-dimensional structures refer to nanomaterials confined in two dimensions, for example,

carbon nanotubes, semiconductor nanowires and long molecules, such as DNA and conducting polymers. Lastly, zero-dimensional nanostructures are confined in all three spatial dimensions. Typical examples include quantum dots, buckyballs, and metal nanoparticles [7].

Compared to microstructures, which typically have similar properties to the corresponding bulk material, nanomaterials are significantly different. The main reasons for this are that nanoscale materials have a large fraction of surface atoms, high surface energy, and spatial confinement [8].

The very large surface area to volume ratio of nanomaterials makes their properties more dependent on their surface compared to bulk materials. This can be used to enhance or modify the properties of the corresponding bulk material. For example, metallic nanoparticles have been used as very active catalysts [9].

Many nanomaterials also have extraordinary thermal and mechanical properties. For example, Chai et al. investigated carbon nanotube reinforced copper nanocomposites and found that the mechanical strength of the nanocomposites was more than three times greater than that of pure copper [10]. The size of nanomaterials is also comparable to the wavelength and mean free path of phonons, so confinement and the resulting quantization makes phonon transport change significantly and results in modified thermal properties. For example, silicon nanowires have much smaller thermal conductivities compared to bulk silicon [11]. Also, high interface densities of nanomaterials have been shown to

reduce thermal conductivity [12]. Conversely, carbon nanotubes have high thermal conductivities due to their unique bonding structure [13].

The electrical and optical properties are determined by electronic states of nanostructures and a great amount of research has been focused on the electrical properties of nanomaterials. For example, space charge spectroscopy [14] techniques have been used to analyze the electrical properties of quantum dots within InAs/GaAs heterostructures. The apparent free carrier concentration and the electronic levels around the quantum dots were investigated [15].

Nanomaterials also have novel optical properties which differ remarkably from bulk crystals due to factors including quantum confinement of electrical carriers, efficient energy and charge transfer over nanoscale distances and in many systems a highly enhanced role of interfaces. Tailoring the crystal dimensions and the chemistry of the surface can control the linear and nonlinear optical properties of nanomaterials. Yao et al. investigated the optical properties of InGaN quantum dots and found that the emission wavelength of quantum dots could be shifted by modifying their dimensions [16].

In addition to the properties mentioned above, nanomaterials have some unique magnetic properties, such as superparamagnetism, which is due to surface disorder, decrease in grain size and an increase in the surface area per unit volume [17]. Magnetic nanomaterials have been used in different applications, such as power generators, motors

for ships, ultra-sensitive analytical instruments, and medical diagnostics and treatments [8].

1.1.4 Biomedical Applications of Nanotechnology

A great amount of biomedical research with nanotechnology has been conducted and shows a promising future [18]. Among these applications nanotechnology provides a wonderful tool for cancer research and can be used widely in the areas of basic science of cancer, cancer diagnostics and treatment. Many countries have invested heavily in cancer nanotechnology. For example, the U.S. National Cancer Institute supports a wide range of cancer nanotechnology research in their Cancer Nanotechnology Plan [19]. In the following sections, biomedical applications of nanomaterials in both diagnostics and treatment will be introduced.

1.1.4.1 Diagnostics

Accurate diagnosis of a disease in its earliest stages is critical for many patients. A great amount of diagnostic methods have been developed in the past, such as ultrasound and analysis of biomarkers. However, these methods are still not sensitive enough and are difficult for the detection of some diseases, such as cancer, at the very early stage. Nanoscale approaches could potentially overcome these challenges.

There are four main nanoscale approaches for the direct imaging of diseases at the cellular and molecular levels: AFM, Transmission Electron Microscopy (TEM), Scanning Electron Microscopy (SEM), and optical methods. Sometimes these methods are combined and used in tandem.

AFM can be used to image a wide variety of cells. Compared to SEM, AFM can image in air or under liquids, and avoids the use of vacuum and high energy electrons. In addition to cells, AFM can be used to image many biological structures, such as DNA, single proteins, and sub-cell structures [20].

Several optical methods, such as near-field scanning optical microscopy (NSOM), fluorescence, and plasmonic methods have been used for nanoscale direct cell imaging. Using NSOM, optical images can be formed with a resolution below the diffraction limit of light. Fluorescence nanoscopy is another optical cell imaging method: A 100 nm three-dimensional resolution can be achieved by this approach in the imaging of protein distribution in the cytosol [21].

Apart from direct imaging, nanoscale biosensors have shown great promise for disease diagnostics. Four types of biosensors will be discussed: biosensors based on optical signals, electrical signals, and structural and magnetic properties.

Optical nanosensors are one of the most recent optical sensor technologies. Like the larger scale sensors, nanosensors have chemical or biological probes [22]. Optical

nanosensors can probe individual cells and detect diseases at molecular and cellular levels. At present, nanoparticles, nanowires, nanotubes, nanoholes, and nanoarrays have been used for optical nanosensors. For example, Kim investigated a nanowire-based surface plasmon resonance which could be used as a biosensor [23].

Electrical nanosensors can also detect diseases at molecular and cellular levels. Compared to fluorescence detection methods, electrical nanosensors are label-free approaches and can avoid the conformational changes caused by the label [24]. Although standard surface plasmon resonance is also a label-free technique, it typically requires complex optical instrumentation that is not suitable for large sensors [24]. At present, biosensors based on nanowires and nanotubes are the two main types of electrical nanosensors. A typical Si-nanowire sensor structure is shown in Figure 1.1: The extremely small cross-sectional area of the Si-nanowire enhances surface sensing. A bias current I_{DS} is measured upon setting a voltage across the drain (D) and source (S) contacts. Changes in surface potential or surface charge cause accumulation or depletion near the sensor surface, and results in a change in the output current of the nanowire sensor [24].

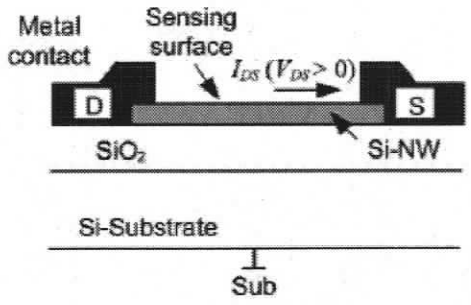

Figure 1.1 Si-nanowire device cross-section which is 20-50 nm in diameter. Adapted from [24].

Nanosensors based on structure and magnetic signals have also shown promise in diagnostics. For example, barcodes store identifying information that can be readily scanned. The image of a barcode can be recorded rather than measuring the light output or other signals. Alternatively, Ruan et al. used quantum dots to generate multiplexed nanobarcodes which could encode genes and detected gene expression changes [25]. Although research on magnetic nanosensors is not as well-developed as optical and electrical nanosensors, some successful studies have been conducted using magnetic nanosensors for biological applications and show promise as tools in cancer diagnostics. For example, Perez et al. developed biocompatible magnetic nanosensors acting as magnetic relaxation switches to detect molecular interactions, such as DNA-DNA, protein-protein, protein-small molecule interactions, and interactions in enzyme reactions [26].

1.1.4.2 Treatment

In addition to diagnostics, a large amount of research shows that nanotechnology can be applied in disease treatment, especially for cancer treatment. Several cancer treatments have been well-developed, such as local surgery, radiation therapy, chemotherapy. Unfortunately all of these techniques have their limitations. Side effects of radiation therapy and chemotherapy are one of the major obstacles for cancer treatment. If cancer cells can be killed without destroying normal cells the life of cancer patients will be extended and their quality of life will be dramatically improved.

Many nanostructures can be used as targeted drug delivery systems, such as liposomes, micelles, nanoparticles, and dendrimers. These nanocarrier systems have some advantages over traditional methods. Associated with nanoscale carriers, the drug volumes of distribution are reduced [27]. The pharmacokinetics and biodistribution of therapeutic agents are also improved [28, 29]. Selective accumulation of drugs at target sites and a much lower concentration in normal cells significantly reduces drug toxicity. Also, the solubility of hydrophobic compounds in the aqueous medium can be improved by many nanocarriers [30]. Finally, the stability of a wide variety of therapeutic agents can be improved by using nanoscale drug delivery systems, such as small hydrophobic molecules, peptides, and oligonucleotides [31, 32, 33].

For treatment applications, an extended circulating time is required for nanoscale drug delivery systems in the blood to increase the chance of passing by tumor cells. For this reason the particle surfaces are usually modified. Polyethylene glycol (PEG) is a hydrophilic polymer and is commonly used due to its low immunogenicity, chemical inertness of the polymer backbone, and availability of the terminal primary hydroxyl groups [18]. Specific targeting of tumor cells is realized by targeting molecules on the particle surfaces. The structure of a PEG surface-modified nanoparticle is showed in Figure 1.2.

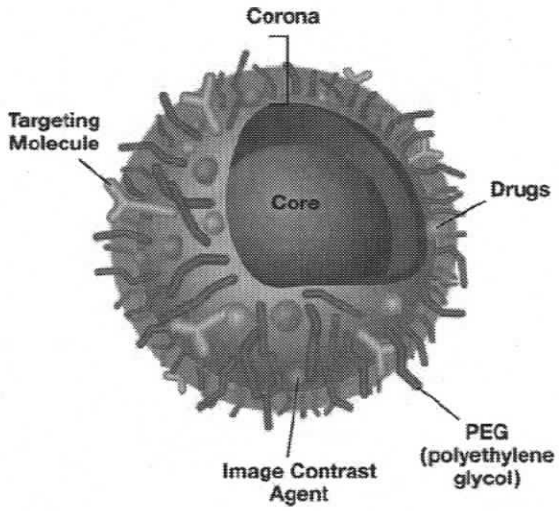

Figure 1.2 Multifunctional nanoparticles. The nanoparticle is modified with hydrophilic polymers, targeting molecules, therapeutic drugs and image contrast agents. Adapted from [18].

In addition to drug delivery, external excitation of nanostructures has also been used for treatment. At present there are generally three types of external excitation used: photodynamic excitation, sonic activation, and magnetic field induced excitation [34].

Photo excitation of functionalized nanoscale materials which can target cancer cells can be used to selectively destroy cancer cells. For example, quantum dots have been reported as potential photosensitizing agents in photodynamic therapy of cancer [35]. Gold nanoparticles also have potential for cancer therapy based on photothermal mechanisms. Light scattering and absorption can be enhanced by their surface plasmon resonance, which leads to local heating and cancer cell destruction [36]. Sonic and ultrasonic activation of nanomaterials can accelerate drug delivery to cancer cells. Crowder et al. developed a general method for augmenting drug deposition locally using ultrasound generated from commercial clinical ultrasound imaging equipment [37]. They

used liquid perfluorocarbon nanoparticles as sensitive targeted drug delivery carriers and applied ultrasound to the nanoparticles. In their in vitro study, lipid delivery from nanoparticles into the cell cytoplasm was dramatically increased.

1.1.4.3 Protein Micro and Nanoarrays

Protein Microarray Formats

Various types of microarrays have been applied in proteomics and disease diagnostics. There are two general types of microarrays: flat microarrays and microfluidic chips. The basic structure and examples of each format will be described below.

Protein microarrays have been applied to analyze specific protein interactions with other proteins, DNA, RNA, ligands and other small molecules, and cells. Initially, scientists developed low-density protein arrays on nitrocellulose filter membranes, for example, the "universal" protein array system which is based on the 96-well microtitre plate format [38]. Lueking et al. improved on this technique and achieved miniaturization by spotting lysates from 92 cDNA (complementary DNA) strands at a density of 600 spots/cm^2 and screened this array of proteins for specific antibodies [39]. Mendoza et al. produced protein microarrays and showed their application for multiplex analysis: They printed proteins on a glass plate that contained 96 hydrophobic Teflon masks. Enzyme-Linked ImmunoSorbent Assay (ELISA) [40] techniques were then used to detect antigens via a charge-coupled device (CCD) detector for imaging of the antigen arrays [41]. One

of the first high-density microarrays was fabricated by De Wildt et al. Their microarrays comprised 18,342 clones [42]. MacBeath and Schreiber investigated spotting proteins and antibodies onto glass slides functionalized with aldehyde groups, which was a breakthrough in terms of protein surfaces [43]. In addition to protein arrays, oligonucleotide chips have also been well developed and provided powerful tools in the Human Genome Project [44]. Protein arrays and biochips directly benefit from this work and have similar large scale efforts, such as the Human Proteome Organization [45]. Thus far, various slide surface materials and surface chemistries have been applied in the fabrication of flat microarrays and some are listed in Table 1.1.

Type	Surface chemistry
Dendrimer slides	Dendrimer layer with reactive epoxy groups
PEG-epoxy slides	PEG layer with reactive epoxy groups
MaxiSorb slides	Polystyrene-based modified surface
Commercially available Amine slides	Amine groups (extended chain length silane)
Epoxy slides	Epoxy groups
Silanated slides	Amine groups
FAST™ slides	Nitrocellulose-based matrix
HydroGel	Modified polyacrylamide gel
Reflective microarray	3-Amino propyl triethoxysilane
Polystyrene cell culture slide	Polystyrene

Aminosilane slides	Amine groups
Quasi monolithic technology epoxy slides	Epoxy groups
Manually prepared slides	
Poly-L-lysine sildes	Amine groups
Polyacrylamide slides	Polyacrylamide

Table 1.1 A list of slide surfaces and their surface chemistry used for protein arrays. Adapted from [46].

Labeled binding molecules or without modification of the binder have been used to detect the molecular interactions on microarrays. Radioactivity and fluorescence are typically used for direct labeling [47]. The radioactive labeling methods have some risks of contamination and problems with waste disposal. On the other hand, the development of bright and pH stable dyes with narrow emission and excitation spectra has enabled the wide use of fluorescent detection methods. The application of several fluorophores simultaneously and the direct comparison and relative quantification can be achieved with commonly used scanners [46]. Different detection methods for antibody and protein microarrays are shown schematically in Figure 1.3. Compared to direct detection, indirect detection does not change the properties of the analyte.

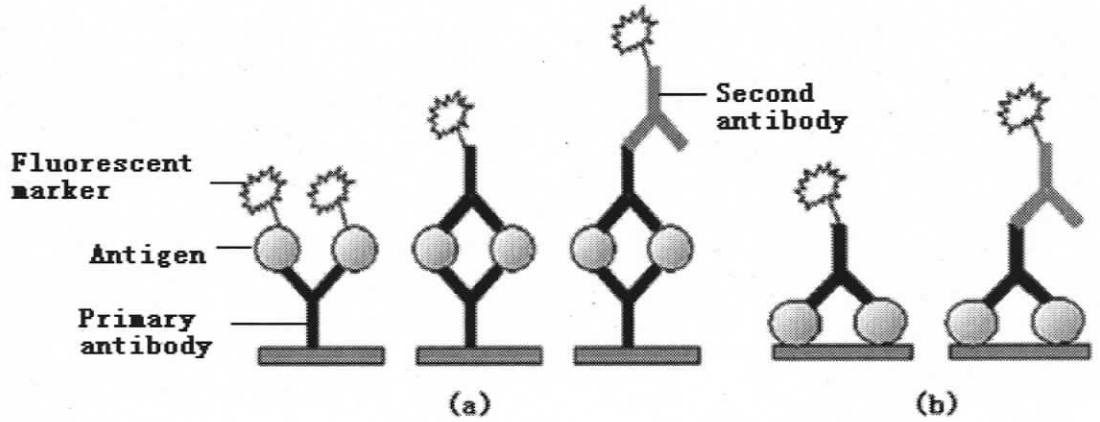

Figure 1.3 (a) Three detection methods for antibody microarrays. (left) fluorescent marker is directly attached to the protein of interest. (middle) indirect labeling of the primary antibody. (right) indirect labeling of the second antibody. (b) Direct and indirect detection of protein microarrays. Adapted from [46].

Several shortcomings exist for flat microarrays: The hybridization process on surface supports requires long incubation times. Also, reproducibility and sensitivity can be lowered due to the cleavage of linkage chemistry of the probe over the extended incubation times [47].

Microfluidics deals with these issues via precise control and manipulation of fluids which are geometrically constrained to a small, usually micrometer scale. On microfluidic chips, microwells are connected by tubing so that liquid handling can be achieved in a miniaturized format [46]. Compared to flat microarrays, microfluidic systems require less reagent cost and have potential for faster detection speed. Since different samples flow in microfluidic systems through separate closed paths, parallel processing is another advantage of microfluidic systems and cross contamination is reduced. However, due to their non-contact mode of spotting and drawing analytes the

implementation and further refinement of microfluidics is still challenging [47]. Both flat microarrays and microfluidic chips are useful methods in the patterning of biomolecules.

Early on, plasma reactive ion etching techniques were used in the fabrication of microfluidic devices. Typically used substrate materials include glass, silicon, and quartz. They have well defined surfaces and excellent optical properties, which are highly required for signal production by optical detection methods. There are some disadvantages for this lithography, such as time consuming, labor intensive and relatively expensive [47]. As alternative substrate materials, polymers (e.g. PDMS) can be used for large scale microfabrication. UV laser ablation, hot embossing, injection molding, or direct micromilling techniques can be applied to create fluidic networks on polymer substrates [47].

Nanoarrays

There is an ongoing trend to reduce the size of devices in both the semiconductor industry and biotechnology industry. For example, more densely packed nanoscale components and faster chips have been developed in the semiconductor industry leading to great advances in information technology [48]. There is a similar drive towards the nanostructuring of protein surfaces. Nanoscale protein arrays have high array densities and thus higher throughput, require less analytes and can potentially reduce the cost of fabrication and analysis.

Although microarrays have been successfully applied in analyzing molecular interactions, such as nucleic acid and protein interactions, and have shown the benefits of miniaturization, microscale bioarrays still have some limitations in many applications. For example, with microarray systems picoliter sample volumes that contain protein analytes, such as cancer biopsy material, still cannot be analyzed and require novel analytical approaches [49]. On the other hand, nanoscale array biosensors can be used in the study of DNA, protein-protein interactions, and protein-cell interactions with better sensitivity and signal quality [50]. A much smaller volume of sample is required. For example, Li et al. utilized gold nanoparticle labeling and silver enhancement to generate nanoarrays to detect target DNA via DNA hybridization [51]. Self-assembled, hexagonal polystyrene-b-poly (vinylpyridine) micelle templates can also be used to create protein arrays with two-dimensional control [52].

1.2 Overview of Thesis

1.2.1 Motivation

Analysis of proteins with a small sample amount, high throughput and a tremendous range of probes can be achieved by miniaturization of protein arrays [53]. Based on this consideration, microarrays have been well-developed and applied for some applications. In recent years, with the development of nanotechnology and biotechnology, protein nanoarray techniques are emerging, and analysis with better sensitivity, high density, and a much smaller amount of sample can be potentially achieved [50]. Some successful

research in protein nanoarrays has shown that the interactions between different proteins, and protein and substrate materials occurs at the nanometer scale and thus nanomaterials are natural structures for future proteomics [43, 54].

Many nanopatterning methods have been developed; however, each of these methods has to overcome certain limitations in order to achieve commercially viable fabrication methods for protein nanoarray biosensors. Achieving large-scale fabrication is still a challenge for most approaches. In addition, the cost of many precise fabrication techniques is quite high. The accuracy of detecting biomolecules needs to be improved, and some issues such as non-specific binding need to be overcome. Speed, flexibility, and control are some other challenges among current fabrication methods.

In this work, we use an inexpensive, fast, and flexible self-assembly method, colloidal lithography, to develop nanometer-scale protein arrays.

1.2.2 Outline

We fabricate nanoparticle arrays with colloidal masks and attach antibody and antigen proteins, which are used as immunological bioassays, and show potential as protein biosensors for many other applications.

The second and third chapters are the main sections of the thesis. The second chapter describes the fabrication of protein nanoarrays with colloidal lithography in detail. The basic mechanism of colloidal lithography is introduced, and the fabrication process used

is demonstrated step by step. Characterization of the protein nanoarrays is covered in the third chapter. Various characterization methods are presented and the data obtained from these methods is analyzed and discussed.

In the final chapter, the main results are summarized and the advantages and limitations of this work are presented. Improvements are proposed and potential applications and future work are described to conclude the thesis.

2 Fabrication of Protein Nanoarrays

2.1 Colloidal Lithography-Background

A colloid is a type of mechanical mixture where one substance is dispersed evenly throughout another [55]. Typically there are two separate phases in a colloidal system: a dispersed phase and a dispersion medium. The dispersed phase particles have at least one dimension which is between 1 nanometer and 1 micrometer.

Through self-assembly colloidal particles can be arranged into well-ordered arrays and be used as masks for the fabrication of advanced functional materials [56]. Colloidal particles in a hexagonally packed array are used as masks for deposition or etching through the mask openings between colloidal particles. For example, e-beam, or a thermal evaporator can be used to generate a nanoscale array of triangular metal dots by direct deposition. The openings between the colloidal particles that are used for deposition or etching allow the formation of relatively small dot arrays compared to the size of the colloidal particles [57].

Compared to other nanolithography methods, colloidal lithography has some distinct advantages. As a bottom-up approach, colloidal lithography is simpler and much cheaper than typical top-down approaches, such as photolithography, electron-beam lithography, and dip-pen lithography. As a self-assembly method, colloidal lithography does not require complex processing, and the colloidal dispersions are commercially available.

Template formation can be achieved via spin-casting or dip-coating, and by changing the size of the colloidal particles and using annealing methods, the feature sizes are easily controlled. Another advantage is that colloidal lithography is suitable for biomaterial patterning, which is the focus of our work.

As mentioned above, colloidal lithography can create nanoscale polygonal dots with sharp edges, which have structure-dependent optical or magnetic responses. For example, Jeong et al. fabricated hexagonal lattice Co/Pd multilayer nanodot arrays using colloidal lithography [58]. Colloidal lithography has also been applied in some biological applications, since metal nanopatterns can be used in applications such as bioanalytical chemistry, bioseparation, and bioimaging [59].

SEM images of monolayer polystyrene masks and gold nanoarrays fabricated using a colloidal mask are shown in Figure 2.1. In addition to nanoparticle arrays, other nanostructures, such as nanometer scale disks, holes, rings, and pores can be fabricated via colloidal lithography. In many applications, the shape of the patterns as well as the feature size is very important to their properties. The shape of colloidal particles can be modified by using post-treatments methods, such as reactive ion etching (RIE), ion milling, and annealing. For example, polymeric particles, such as polystyrene and PMMA, exhibit a glass transition at elevated temperatures. Modification of a colloidal mask by thermal annealing and rotational tilted deposition through the annealed mask is shown in Figure 2.2.

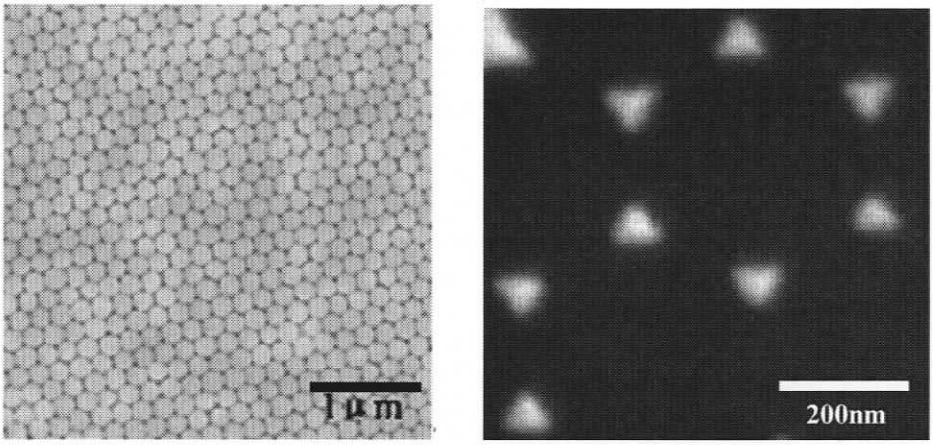

Figure 2.1 SEM images of nanosphere masks (left) and nanoparticle arrays (right). Adapted from [60, 61].

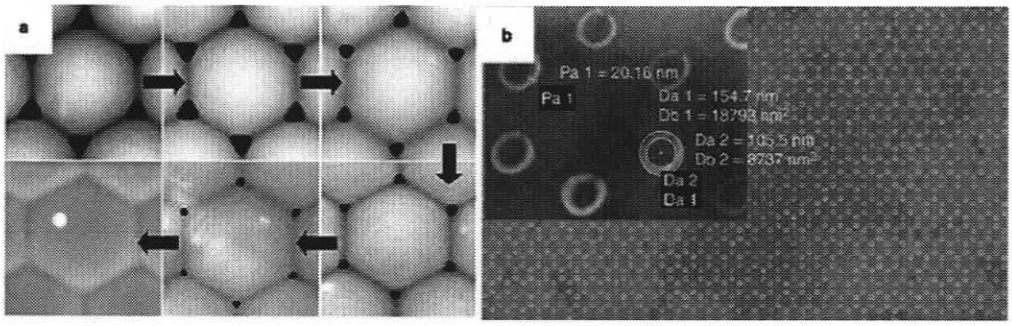

Figure 2.2 Modification of a colloidal mask by deforming the colloidal array. (a) the size of the openings is controlled by the annealing. (b) Nanoring structure fabricated by rotational tilted deposition through the annealed colloidal mask shown in (a). Adapted from [62].

2.2 Fabrication Process

The entire protein nanoarray fabrication process we employed is summarized in Figure 2.3. Polystyrene nanosphere solution is dropped onto the substrate surface and forms monolayer masks. Gold nanoparticle arrays are formed via metal deposition and removal

of the nanosphere masks. IgG molecules are then attached through chemical surface modification of the gold nanoparticles. Lastly, specific attachment of anti-IgG molecules onto IgG monolayers tests the bioactivity of the protein arrays.

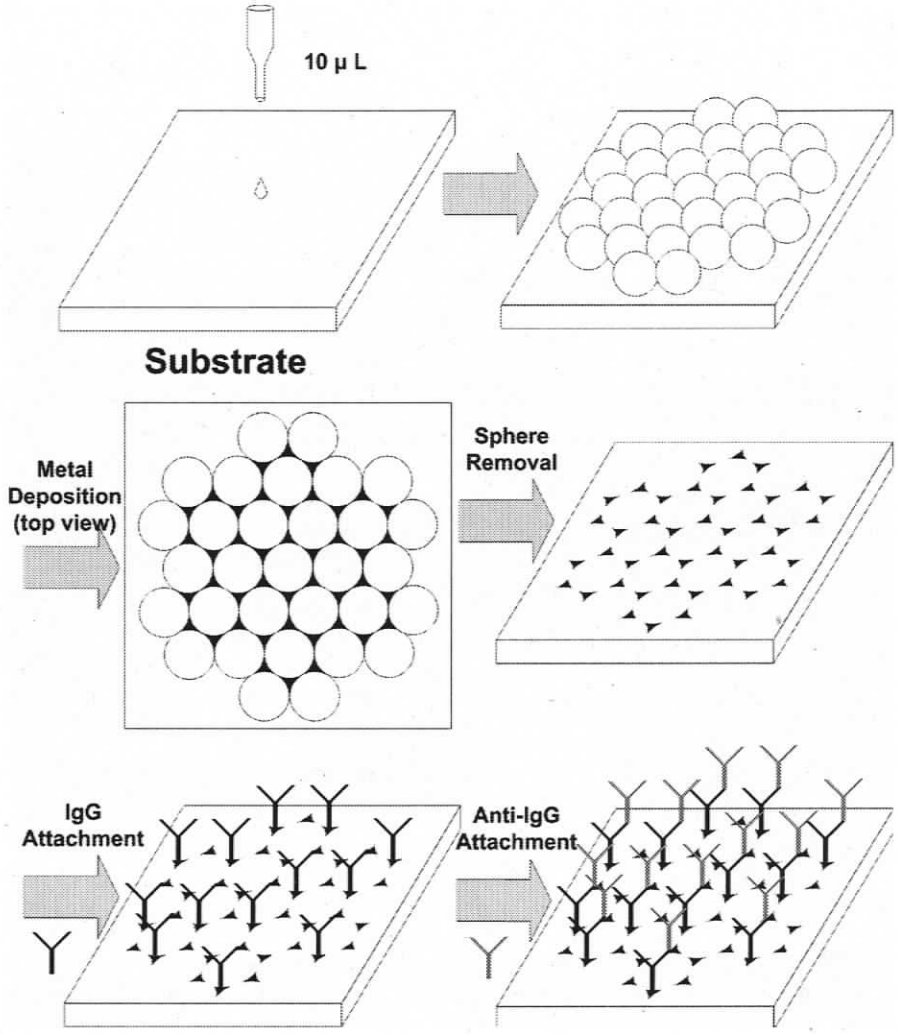

Figure 2.3 Protein Nanoarray Fabrication Process. 1: Formation of monolayer masks. 2: Formation and exposure of nanoparticle arrays via metal deposition and sphere removal. 3: Monolayer IgG attachment and test of bioactivity of protein arrays by attaching anti-IgG molecules.

2.2.1 Formation of Metallic Nanoparticle Arrays

2.2.1.1 Substrate Materials

There are some general considerations for choosing the substrate materials on which the nanoparticle arrays are formed using colloidal lithography including flat, clean surface properties, versatility in terms of chemical modification, and low cost [63]. Also, a flat surface is important for analyzing nanoarrays with precise scanning methods [63]. Various substrates have been applied for the fabrication of nanoparticle arrays, including silicon, glass, quartz, mica, plastics, gold, aluminium, and indium-tin oxide [64, 65]. Among these materials, silicon, glass, and mica are some of the most commonly used for nanoarrays and are also widely used as substrates for biological micro and nanoarrays, including both DNA arrays and protein arrays.

In this work, we used silicon, glass, or mica as the substrate materials for the fabrication of nanoparticle arrays and subsequent protein attachment. The substrate materials used are listed below:

- VWR microscope cover glass: 25x25 mm (square), 0.17-0.25 mm thick;
- VWR microscope cover glass: 18 mm (circle), 0.13-0.17 mm thick;
- VWR microscope cover glass: 22 mm (circle), 0.13-0.17 mm thick;
- Silicon Quest International silicon wafer: n-type (P dopant), 500-550 μm thick, <100>, resistivity 10-20 Ω-cm;
- SPI Supplies mica: grade IV/V, 0.15 mm thick.

2.2.1.2 Formation of Colloidal Sphere Monolayers

Substrate Pretreatment

Pretreatment of the substrates before the formation of colloidal sphere monolayers is often critical. The purpose of pretreatment steps is usually to render the surface hydrophilic and improve its wettability [66]. In our work, we used sonication in ethanol and acetone to clean the surface of the glass cover slips. After sonication, the cover slips were rinsed thoroughly with deionized water (DI H_2O). To test that these pre-treatments improve the surface wettability, we made a comparison of sonicated and non-sonicated samples [67] and images obtained with an optical microscope are shown in Figure 2.4. The nanosphere solution dropped onto a cover slip with no sonication did not spread out as well and formed a very thick area of multi-layer nanospheres. We typically found that the ethanol sonication treatment produced better monolayer surfaces than those sonicated with acetone [67].

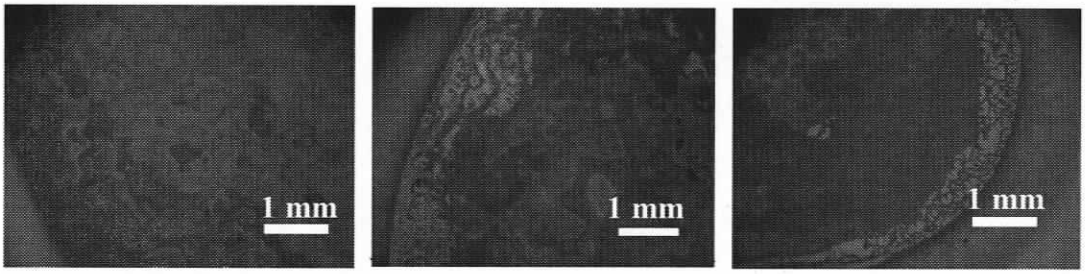

(a) (b) (c)

Figure 2.4 Nanospheres on glass slides after drying. (a): no sonication, (b): acetone sonication, (c): ethanol sonication. Adapted from [67]. Orange regions are monolayers.

In addition to sonication methods, we also used Contrad 70 to clean the substrate surfaces. Contrad 70 is a laboratory strength cleaning solution manufactured by Decon Laboratories Limited. To prepare the cover slips, we first placed the cover slips in isopropanol solution and boiled them on a hot plate for a few minutes. The cover slips were removed from the isopropanol and allowed to dry in air for one minute. Next, the cover slips were placed in a warm beaker of 2% Contrad 70 (in DI H_2O) and warmed for approximately 2 hours over the hot plate. The cover slips were then removed from the Contrad solution and rinsed thoroughly with DI H_2O and dried [67]. Silicon substrates were pretreated using similar methods. Mica needed only to be freshly cleaved before use.

Self-assembly of Nanospheres

After substrate pretreatments, colloidal nanosphere solutions were used to form monolayer masks. The nanosphere material we used was polystyrene. The chemical structure of the polystyrene molecule is a long chain hydrocarbon with every other carbon connected to a Phenyl group, as shown schematically in Figure 2.5.

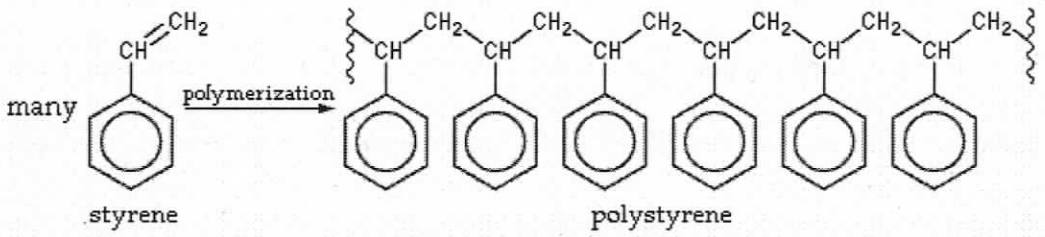

Figure 2.5 Polystyrene structure.

The nanospheres used were purchased from Interfacial Dynamics Corporation (surfactant-free white carboxyl latex) with diameters of 450 nm and 720 nm. The solid percentage was 4.0 and 3.8 respectively and the coefficient of variation of diameter was 1.1% and 2.1% respectively. Also, we used another batch of the same type of spheres with 450 nm and 780 nm diameters, and solid percentages of 4.0 and 4.2 and coefficient of variation of diameter of 1.1% and 3.2%, respectively. The aqueous nanosphere solutions were dropped onto the various substrates and then allowed to dry and assemble into hexagonal close-packed arrays. An example of a resulting monolayer is shown in Figure 2.6. Although there are other ways to increase sphere coverage, simple drop-coating as used here is a straightforward approach that allows the proof-of-concept that we require to be demonstrated.

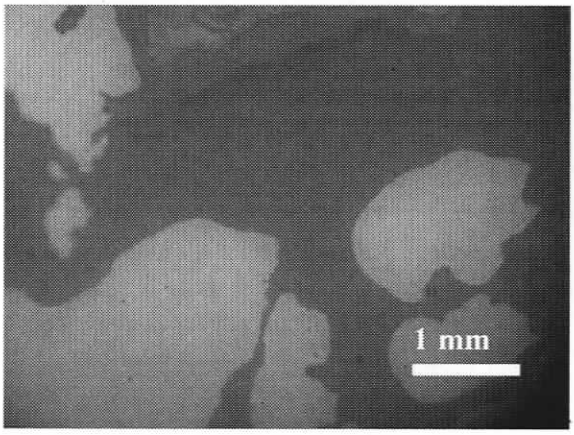

Figure 2.6 Nanospheres on glass substrate pre-treated by Contrad 70. Adapted from [67]. Orange areas are monolayers, whose color depends on the size of nanospheres and substrate materials.

We found silicon was the most difficult substrate for creating large monolayers of nanospheres. The mica substrate was freshly cleaved into thinner mica sheets. Pure nanosphere solutions were dropped onto the cleaved mica and then allowed to dry in air or in a nitrogen desiccator to form large monolayers with large domains. Optical images of samples prepared from glass, silicon, and mica are shown in Figure 2.7.

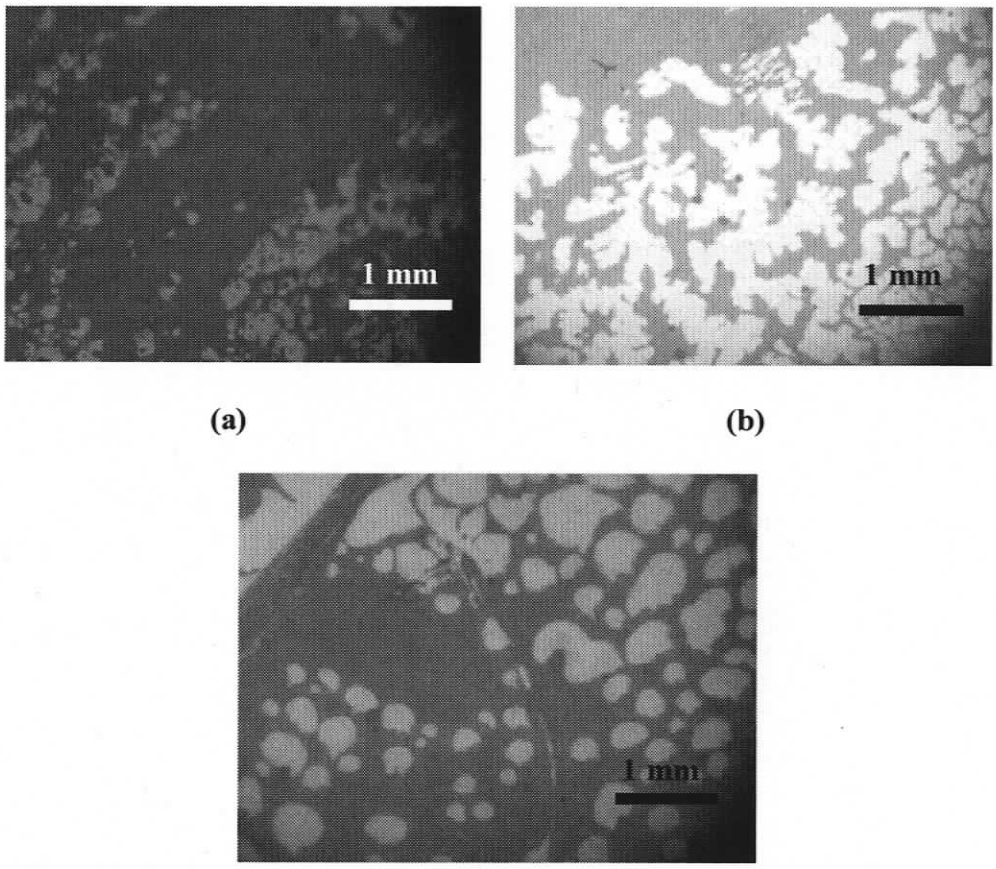

Figure 2.7 780 nm nanospheres on glass (a), silicon (b), and mica (c). Adapted from [67]. Although the size of nanospheres are the same, monolayers showed different colors on different substrates. There are some large domains on glass and mica, and typically fewer on silicon.

Annealing

To control the sizes of the mask openings, we used thermal annealing after formation of nanosphere monolayers. Through annealing, the mask openings can be reduced down to 10 nm or less.

Thermal annealing was performed using a mechanical convection oven. The samples were placed on a glass Pyrex dish and placed in the oven for the allocated time once the oven temperature had stabilized. From previous annealing experiments [68], the optimum annealing temperature was found to be approximately 105°C and typical annealing times were between 100 and 500 minutes for the spheres used in our studies.

2.2.1.3 Metal Deposition

Once the colloidal masks were formed, metal deposition was carried out using an e-beam evaporator. A layer of titanium was evaporated on the surface to increase the adhesion. The thickness of titanium was ~5 nm. Following the adhesion layer, gold of thickness ~35 nm was deposited. To decrease the roughness of gold nanoparticles, relatively high evaporation rates were used [69][1].

[1] We thank Ph.D. candidate Badr Omrane for his technical support with the metal deposition.

2.2.1.4 Sphere Removal

The last step to form nanoparticle arrays is to remove the nanospheres and expose the nanoparticle arrays. In our work, we removed the spheres by sonication in pure ethanol for 3-5 minutes. Figure 2.8 shows a glass sample after sonication.

Samples were rinsed in ethanol and DI water after sphere removal. After rinsing, the samples were dried under N_2 stream and were ready for further processing.

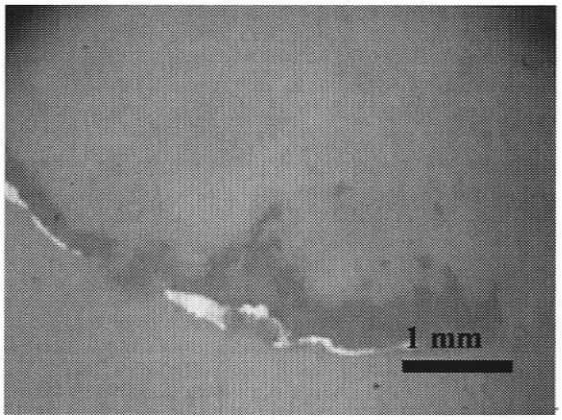

Figure 2.8 Gold-on-glass sample after sonication in pure ethanol. Most monolayer spheres are removed.

2.2.2 Surface Modification of the Nanoparticle Arrays

2.2.2.1 Overview of the Surface Modification Process

Compared to bulk metals, metal nanoparticles are easier to modify with different chemicals [18], which enables applications in biological and medical research. There are many methods to modify gold nanoparticles for protein attachment [70, 71]. In this work, we modified gold nanoparticles with mixed COOH-terminated self-assembled monolayers (SAM) and N-hydroxysuccinimide (NHS) chemistry in order to have a high affinity towards the desired proteins. Figure 2.9 shows a schematic of the modification of the nanoparticle surfaces we employed. COOH-terminated alkanethiol self-assembled monolayers (3-MPA and 11-MUA) are attached onto gold nanoparticles, followed by attaching the NHS group to the COOH terminus. Proteins are covalently bound onto gold nanoparticles by replacing the NHS groups with the N-terminus of the proteins.

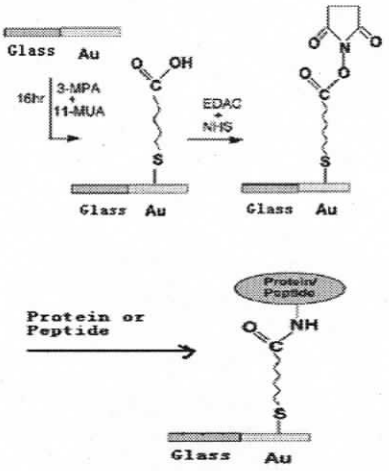

Figure 2.9 A schematic representation of chemical reaction schemes for coating the patterned surface with proteins or peptides on gold nanoparticles. Adapted from [72]. Thiol self-assembled monolayers and NHS/EDC are used to covalently bind proteins onto gold nanoparticles.

SAM Formation

Self-assembled monolayers are simple to use and can control biomolecule surface orientation. This allows SAMs to play an important role in the construction of artificial biomolecular recognition surfaces and in the development of biosensors [72]. The formation of such self-assembly monolayers is very versatile and is a widely used surface functionalization method in the development of biosensors that can mimic naturally occurring recognition processes at molecular level [73]. Sulfur-containing SAMs include alkanethiols, dialkyl disulfides and dialkyl sulfides. They have a strong affinity for noble metal surfaces [74] and are very commonly used SAMs. For alkanethiols, the binding mechanism involves an oxidative addition of the S-H bond reaction, followed by reductive hydrogen elimination, leading to the formation of thiolate species. Molecular hydrogen is formed by the combination of the eliminated hydrogen, as described in Eq. 1 [75, 76].

$$R\text{-}S\text{-}H + Au_n^{\circ} \rightarrow R\text{-}S\text{-}Au^{+} \cdot Au_n^{\circ} + 1/2\ H_2 \quad (1)$$

Kinetic studies of alkanethiols bound to gold surfaces showed that this process occurs in two distinct phases: an initial fast phase and a second slower phase [77]. In the fast phase the sulfur-containing compound is assembled onto the metal substrate. In the slower phase the alkyl chains rearrange and van der Waals interactions produce an extended close-packed conformation. It is found that the alkyl chains are not

perpendicular to the gold surface. There is an angle between 26° and 28°, as shown in Figure 2.10 [77].

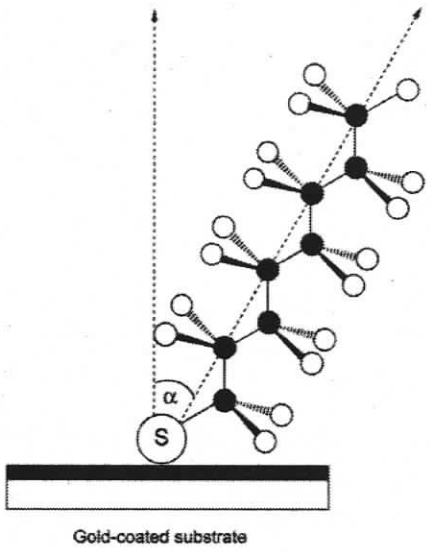

Figure 2.10 Tilt of the alkyl chain of a SAM molecule away from the perpendicular to the gold. Adapted from [77]. The angle α is between 26º-28º.

In this work, we used 11-mercaptoundecanoic acid (11-MUA) and 3-mercaptopropionic acid (3-MPA) monolayers. These two compounds were used to produce hydrophilic SAMs, terminated with carboxylic acids which were then further modified. The chemical formula of 11-MUA is $(CH_2)_{11}O_2S$, and the molecular weight is 218.35 g/mol. The chemical formula of 3-MPA is $(CH_2)_3O_2S$, and the molecular weight is 106.14 g/mol. The structures of 11-MUA and 3-MPA are shown in Figure 2.11.

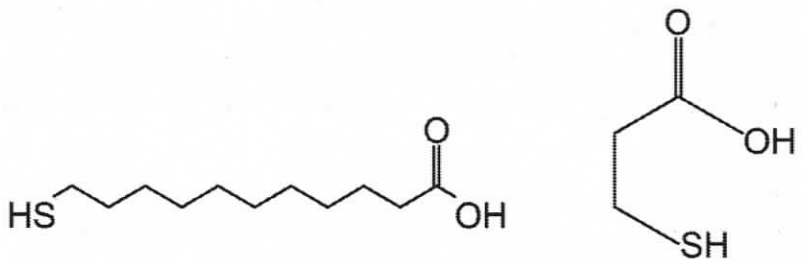

Figure 2.11 Structures of 11-MUA (left) and 3-MPA (right).

NHS/EDC

NHS is a slightly acidic compound that is used as an activating reagent for carboxylic acids. The molecular formula of NHS is $C_4H_5NO_3$ and the molecular weight is 115 g/mol. Activated acids can react with amines to form amides. To form a highly unstable activated intermediate, a dehydrating agent, in our work 1-ethyl-3-(3-(dimethylamino)propyl)carbodiimide (EDC), is added into NHS solutions. EDC is a crosslinking agent. It can be used to couple carboxyl groups to primary amines. The molecular formula of EDC is $C_8H_{17}N_3$-HCl and the molecular weight is 191.7 g/mol. EDC is a widely used crosslinker. Its applications involved forming amide bonds in peptide synthesis, labeling nucleic acids through 5' phosphate groups and creating amine-reactive NHS-esters of biomolecules. An amine-reactive intermediate can be formed through the reaction between EDC and a carboxyl. With NHS, EDC is used to convert carboxyl groups to amine-reactive NHS esters [78]. The structures of NHS and EDC are shown in Figure 2.12. NHS reacts with SAMs to form a less labile activated acid [78].

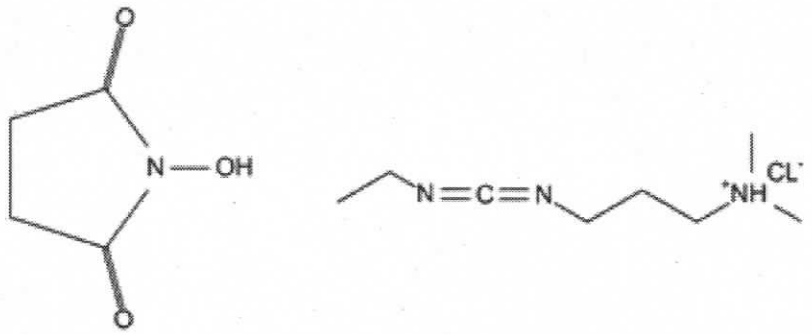

Figure 2.12 Structures of NHS (left) and EDC (right).

Proteins Used for Attachment

IgG is a tetrameric immunoglobulin that is built of two heavy chains and two light chains [79]. As an antibody, each IgG molecule has two antigen binding sites. IgG is the most abundant immunoglobulin in animal bodies. IgG antibodies have 4 peptides and are relatively large molecules. Disulphide bonds connect two heavy chains and also link the two heavy chains to a light chain each. The tetramer has a Y-shape. Two antigen binding sites are at the end of the Y-shaped fork [80]. Y-shaped IgG has a height of 14.5 nm, a width of 8.5 nm and a thickness of 4.0 nm. Anti-IgG (anti-Immunoglobulin G, reacts with corresponding IgG) molecules have similar structures to IgG molecules [54]. The 2-D schematic and 3-D structure of an IgG molecule are shown in Figure 2.13.

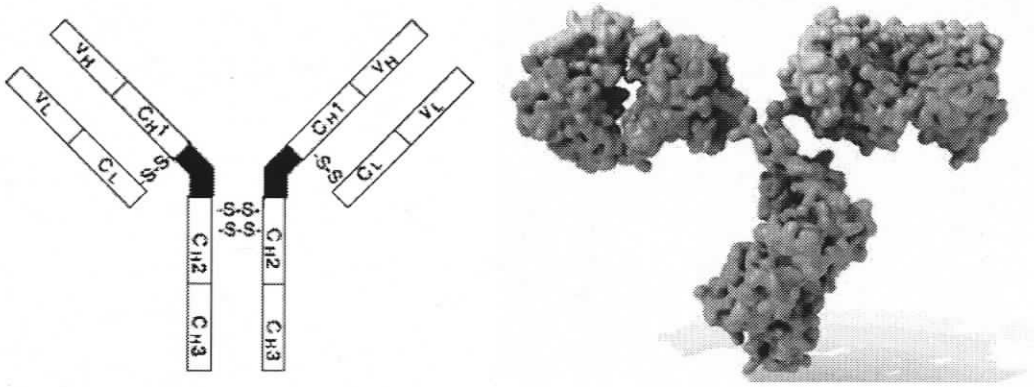

Figure 2.13 IgG molecule composed of two light (L) and two heavy (H) chains held by disulfide bonds. (left): 2-D schematic of an IgG molecule. (right): 3-D structure of an IgG molecule. Adapted from [79, 81]. IgG has a height of 14.5 nm, a width of 8.5 nm and a thickness of 4.0 nm [54].

2.2.2.2 Experimental Procedures

SAM Formation

COOH-terminated alkanethiol monolayers on the substrates were formed by soaking the substrates with nanoparticle arrays for 18 hours in 20 mM ethanolic solutions of mixed MUA/MPA (1:10 v/v). At this molar ratio of SAM, thiols are more reactive towards proteins than other ratios [82]. The materials we used for the SAM formation are listed below:

11-mercaptoundecanoic acid (11-MUA): $C_{11}H_{22}O_2S$, 95%, Sigma-Aldrich;

3-mercaptopropionic acid (3-MPA): $HSCH_2CH_2COOH$, 99%, Sigma-Aldrich.

After soaking in SAM solution, thorough rinsing is critical to remove physically adsorbed residues. In our early trials, we rinsed the samples with ethanol for 20-30

seconds, and then thoroughly rinsed with DI water. However, after scanning the samples with AFM (see Chapter 3) we found that there were some SAM residues remaining on the glass substrates. Therefore, we increased the amount of rinsing: 30 seconds with ethanol; soaking in ethanol solution for 30 minutes, and repeat. After briefly rinsing once more with ethanol, the samples were finally rinsed thoroughly with DI water.

NHS/EDC

After processing the samples as described above, we immediately continued with the next step. NHS and EDC were used to further modify the substrates: Next, we immersed the substrates with carboxylic acid-terminated SAMs in an aqueous solution of 75 mM EDAC and 15 mM NHS for 1 hour to attach the NHS group to the COOH terminus. The solution containing NHS and EDC was prepared immediately prior to use. It was reported that using this method, the subsequent orientation of proteins was improved compared to previous protein attachment methods [72]. The materials we used for this step are listed below:

N-hydroxysuccinimide (NHS): $C_4H_5NO_3$, 98%, Sigma-Aldrich;

1-ethyl-3-(3-(dimethylamino)propyl)carbodiimide-HCl (EDAC-HCl): $C_8H_{17}N_3$-HCl, Sigma-Aldrich.

Similar to the previous step, rinsing is critical following the NHS/EDC coupling. The samples were rinsed with DI water for 30 seconds, soaked in DI water for 3 minutes, and then rinsed with DI water for another 20 seconds.

IgG Attachment

After NHS/EDC surface modification, we attached proteins on the substrates. We used IgG and anti-IgG molecules as a typical immunological model to show that our nanoparticle arrays can be used for immunoassays [83].

The materials we used are listed below:

Normal Rabbit IgG: 3mg/mL, Caltag Laboratories

PBS: 1X solution, 11.9 mM Phosphates, 137 mM Sodium Chloride, 2.7 mM Potassium Chloride, pH: 7.4±0.1, FisherBiotech.

The proteins were preserved in a freezer to maintain their bioactivities. 1-2 days before making protein solutions, the proteins were thawed in a refrigerator at ~5ºC.

To make the protein solutions, we used phosphate buffered saline (PBS) solution. PBS is widely used in biological research and it is a salty solution that helps maintain a constant pH value in solution. The osmolarity and ion concentrations of PBS solution are suitable for biological substances [84]. The pH value and concentration of the PBS buffer are two important considerations: The wrong pH will affect the bioactivities of proteins; Unsuitable concentrations of PBS will destroy the structure of protein molecules.

In this work, we used PBS buffer solution with a pH value 7.4±0.1 at room temperature, and a phosphate concentration of 11.9 mM. The protein concentration we used to prepare both rabbit IgG solutions and goat anti-rabbit IgG solutions was 20 μg/mL. The

concentration of proteins is important because a high concentration may lead to large protein aggregation, producing a large amount of background noise. On the other hand, a low concentration of proteins may lead to difficulties for protein attachment onto gold.

When the IgG solutions were ready, the substrates modified in the previous steps were soaked in the protein solution for 1 hour. Proteins were covalently bound on the substrates by replacing the NHS groups with N-termini protein residues, as shown in Figure 2.9.

After IgG attachment, a thorough rinse is critical to remove unwanted protein residues and to avoid non-specific binding and decrease background noise. Non-specific binding is a common issue for nanometer-scale protein arrays (and biomolecular arrays in general). In our work this refers to binding of IgG molecules on the substrate to places other than gold.

There are many rinsing approaches to reduce non-specific binding. For example, some scientists rinse substrates with PBS solutions and DI water; while others use PBS solution, Tween-20, and DI water to reduce non-specific binding of proteins [85]. In this work, we rinsed the samples after each protein attachment for 30 seconds with DI water, and soaked the samples in DI water for 5 minutes. Then the samples were rinsed with flowing water for 3 minutes, and rinsed with DI water for 30 seconds. After this thorough rinsing, the samples were dried in a stream of N_2, and stored in a N_2 desiccator at room temperature.

Anti-IgG Attachment

In order to test the bioactivity of the IgG arrays, the samples were immersed into a PBS buffer solution of goat anti-rabbit IgG molecules (1mg/mL, Invitrogen) for 1 hour at room temperature following IgG attachment. After rinsing as described above, the samples were dried under a stream of N_2 and stored in a N_2 desiccator. The attachment of an anti-IgG molecule onto an IgG molecue is shown schematically in Figure 2.14.

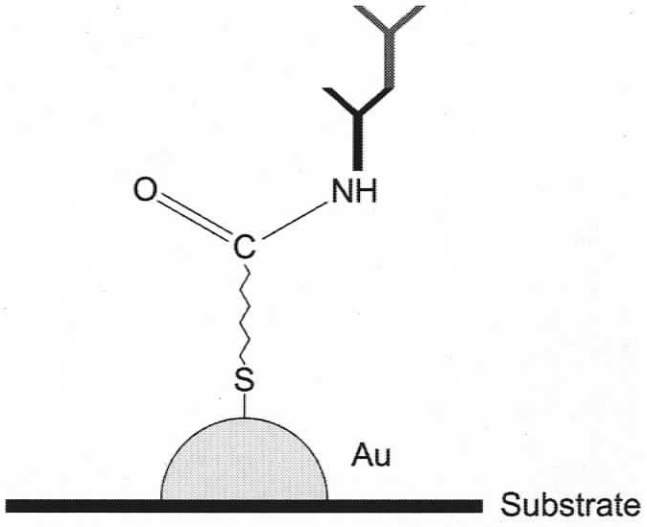

Figure 2.14 Detection of anti-IgG molecules using IgG nanoarrays. Anti-IgG molecules are attached onto the binding site of the IgG molecules (the schematic is not drawn to scale).

2.3 Summary

In this chapter the fabrication of protein nanoarrays using colloidal lithography was described. To form the nanoarrays, we dropped a suspension of polystyrene colloidal spheres onto various surface and self-assembly resulted in a 2D hexagonally close-

packed array that served as a deposition mask. After depositing an adhesion layer, a gold or silver thin film was evaporated onto the colloidal mask. Removal of the colloidal mask exposed the nanoparticle arrays for surface modification. Mixed COOH-terminated self-assembled monolayers (3-MPA+11-MUA) and NHS/EDAC were used to modify the substrates and allowed for covalent coupling of proteins. IgG solutions with a concentration of 20 μg/mL in PBS buffer with pH=7.4 at room temperature were used for protein attachment. Bioactivity of the protein nanoarrays was tested by attaching goat anti-rabbit IgG molecules onto the IgG modified surfaces.

In the next chapter, the protein nanoarrays will be characterized via AFM and SEM and analyzed.

3 Characterization of Protein Nanoarrays

AFM and SEM were used to characterize the protein nanoarrays. The AFM images were collected with a Nanonics MultiView-1000 scanning probe microscope in intermittent contact mode. The software used to analyze AFM images was WSxM, obtained from Nanotec Electronica. The SEM images were collected with a Hitachi S-4700 field emission microscope.

3.1 Characterization of Nanoarrays via AFM

3.1.1 Characterization of Gold Nanoparticle Arrays

Figure 3.1 shows AFM images of a typical gold nanoparticle array on glass before functionalization. This array was obtained from monolayer nanospheres with a diameter of 780 nm, and the masks were annealed at 105 ºC for 300 minutes. There were a large amount of gold nanoparticles on the glass substrate, since the polystyrene nanospheres were spread nicely and formed large monolayer areas. The hexagonal structure of the triangular dots is evident. In Figure 3.1 (b), a close-up image is shown. Figure 3.1 (c) shows a cross-section analysis of the gold nanoparticle vertical and lateral size corresponding to (b). The height of the nanoparticles is approximately 40 nm on average as expected from the evaporation conditions, and the width is about 150 nm (taking into account the smearing caused by the finite radius of the AFM tip).

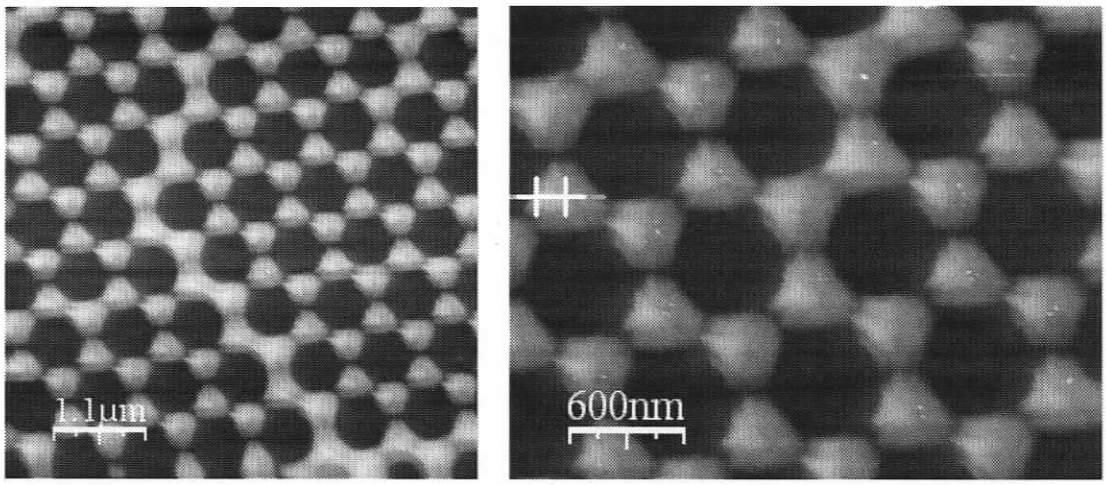

(a) (b)

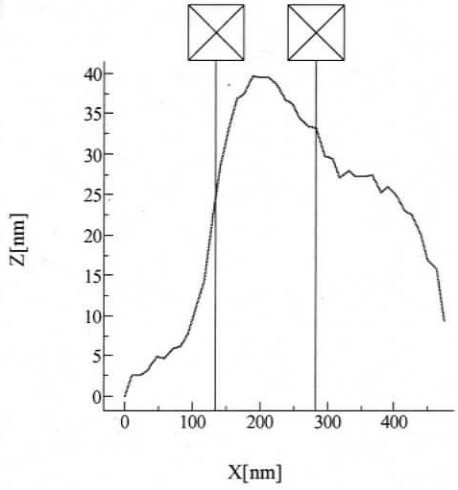

(c)

Figure 3.1 AFM images of gold nanoparticle arrays and cross-section height analysis of gold nanoparticles. (a) Well-ordered gold nanoarrays with hexagonal close-packed structures. (b) Magnified AFM image of gold nanoarray. The nanoparticles have a triangular shape. (c) Cross-section analysis of gold nanoparticle indicated in (b). The height is approximately 40 nm and the diameter is approximately 150 nm. The apparent width is much larger due to convolution of the AFM tip.

Figure 3.2 shows AFM images of a gold strip caused by a defect in the colloidal mask. Figure 3.2 (b) shows height differences across the strip, along the line indicated in Figure

3.2 (a). The height differences in Figure 3.2 (b) imply that there is about 3.5 nm roughness of the gold surface. To improve the flatness, we increased the evaporation rate during metal deposition. Figure 3.2 (c) is an image of an improved sample. The gold surface is much flatter and the height difference across the gold surface is ~1 nm (Figure 3.2 (d)).

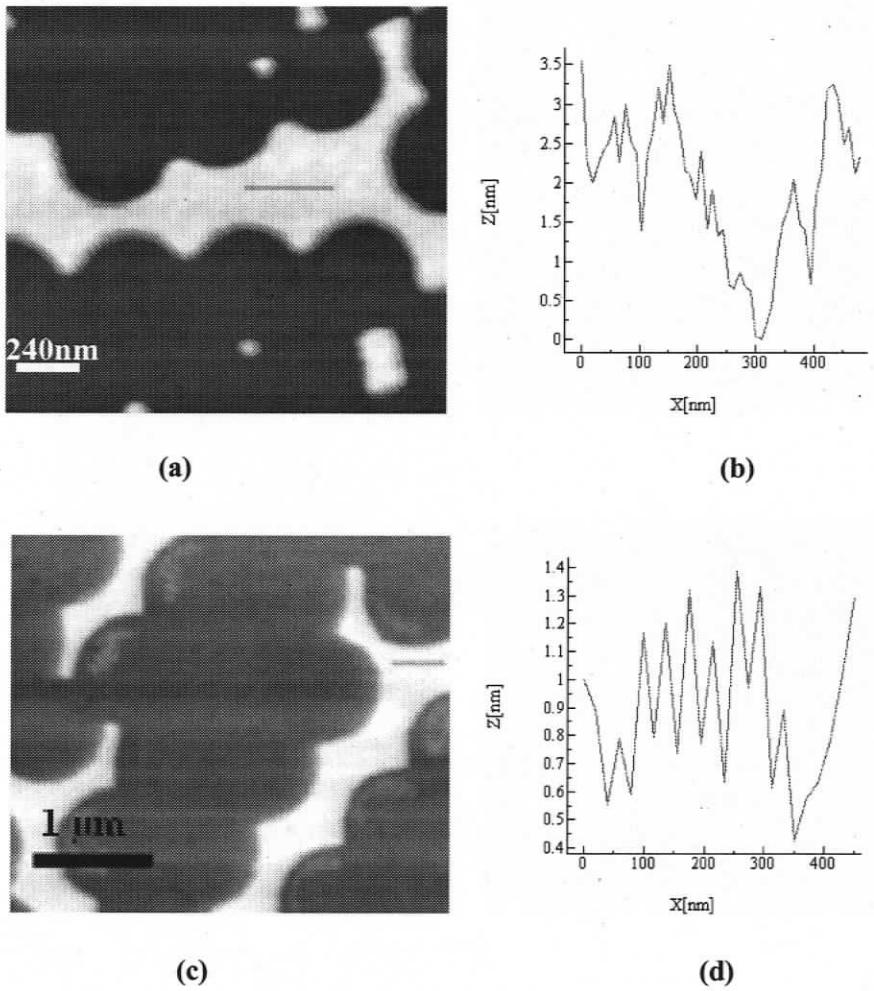

Figure 3.2 (a): AFM image of a gold strip. (b): The height difference between two points on the gold strip in (a) reaches 3.5 nm. (c): Gold strip on a sample with improved roughness. (d): The height difference between two points on the gold strip in (c) is ~1 nm.

3.1.2 Characterization of SAM/NHS Functionalized Nanoarrays

Figure 3.3 shows AFM image of gold line defect after functionalization by SAMs and NHS. The height of the gold is approximately 41.5 nm. The increase in height of 1-2 nm, is consistent with the addition of SAM/NHS. It is also clear from this image that the gold dots in the array are missing after chemical processing. This adhesion issue will be addressed below.

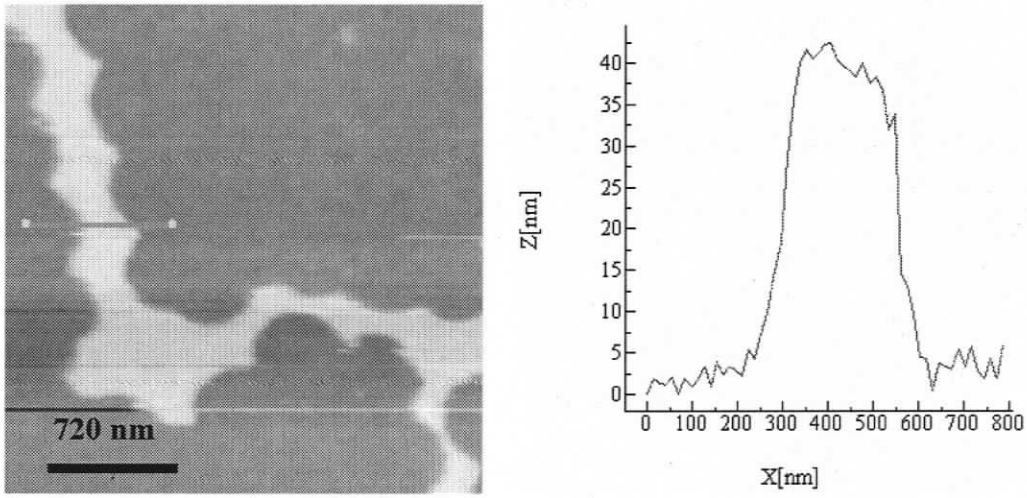

(a) (b)

Figure 3.3 AFM image of SAM/NHS functionalized gold. (a): AFM image of functionalized gold surface. (b) Height analysis shows that the height of gold/SAM/NHS is about 41.5 nm.

3.1.3 Characterization of IgG Protein Arrays

The images in Figures 3.4 - 3.8 were taken from gold on glass samples. Figure 3.4 is a close-up scan of a gold strip after IgG molecule attachment. In Figure 3.4 (a), the IgG

molecules are clearly visible on the gold surface. In Figure 3.4 (b), the height of the film is shown to be about 46 nm. As discussed further below, this indicates a single layer of IgG molecules has attached to the gold surface. In Figure 3.4 (c), the height reaches 60 nm, which implies that likely multiple-layer protein molecules were attached. Non-specific binding of IgG molecules on the glass substrate is also observed in the AFM images, implying that rinsing may have been insufficient for these samples.

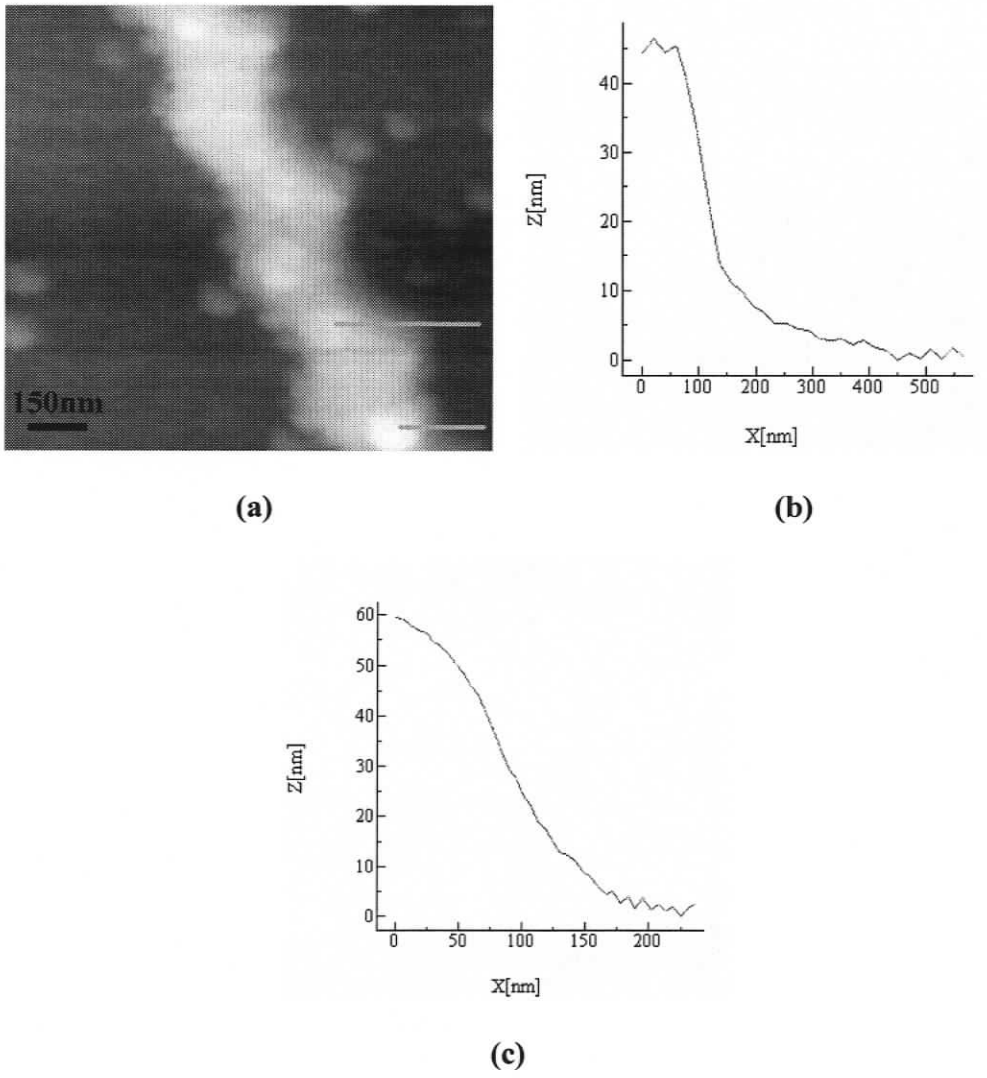

Figure 3.4 (a): AFM image of a gold strip showing IgG attachment onto gold strip. (b): Height analysis corresponding to the upper line in (a) indicates a height increase of 6-8 nm (c): Height analysis corresponding to the lower line in (a) shows a height increase of ~20 nm.

In Figure 3.5, we have a closer look at an individual protein region. In Figure 3.5 (b), the cross-section shows the height of a SAM/NHS "island" and an individual IgG molecule. Larger protein aggregations are also evident.

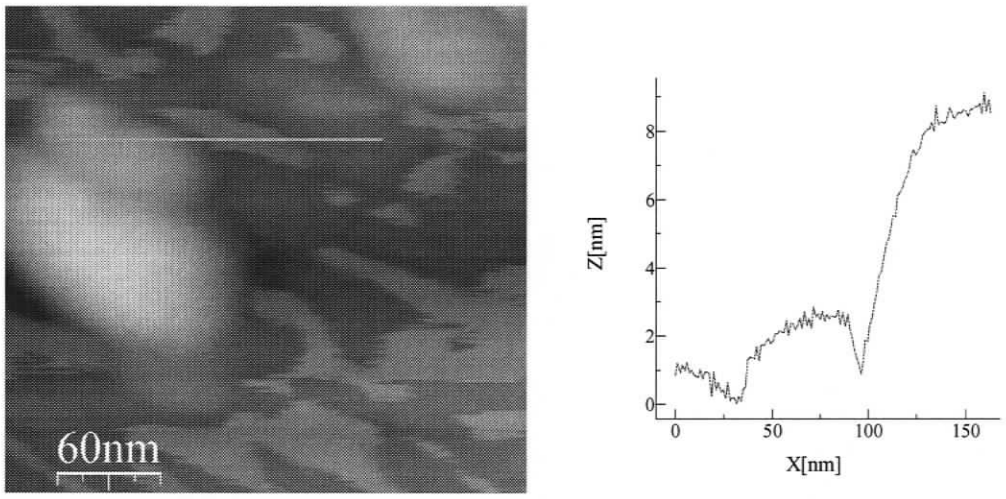

(a) **(b)**

Figure 3.5 AFM image and analysis of proteins and SAM. (a) AFM Image shows individual IgG molecule and aggregation. (b) Height analysis of the protein and SAM layers.

Figure 3.6 shows AFM of several IgG molecules on the glass substrate. In Figure 3.6 (a), the Y-shape of these molecules is consistent with the shape of the rabbit IgG antibodies we used. Figure 3.6 (b) indicates that the height of these molecules is around 7.5 nm. Interestingly, we observe in several AFM images that the protein molecules have the same orientation over large areas. Assuming the proteins are attached onto SAM/NHS layers, this consistent orientation among each IgG molecules shows that this surface functionalization method renders reliable protein orientations, as discussed in reference [72].

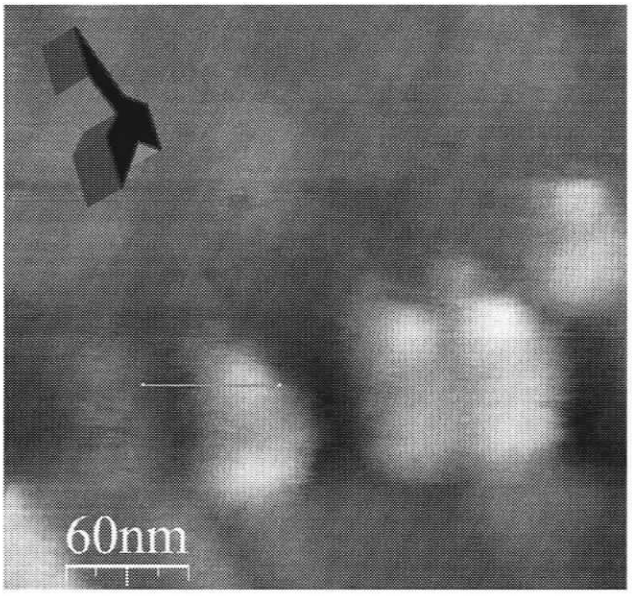

(a)

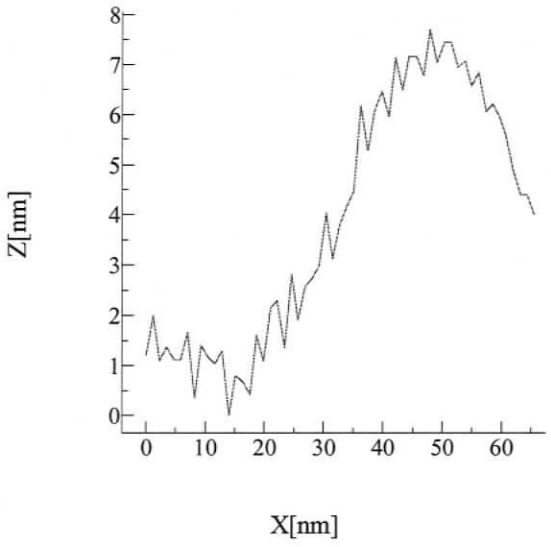

(b)

Figure 3.6 AFM images and analysis of IgG molecules. (a): 2-D image of IgG molecules. All molecules have the same orientation. Inset illustrates possible antibody orientation. (b): Height analysis shows a height of 7.5 nm.

Samples with Improved Rinsing and Adhesion

Figure 3.7 shows AFM images of IgG attachment on gold nanoparticles for glass substrate samples with more thorough rinsing and an improved titanium adhesion layer. The gold nanoparticles have now remained in place after protein attachment. Non-specific binding was also decreased in these samples due to better rinsing. The height data show that there is an increase in height of 6-8 nm compared to bare gold dots, which is consistent with a single monolayer of IgG molecules.

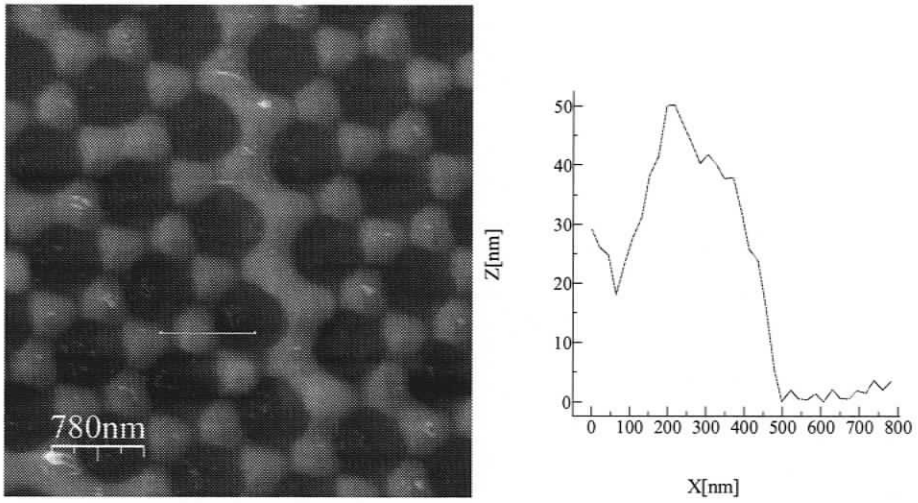

(a) **(b)**

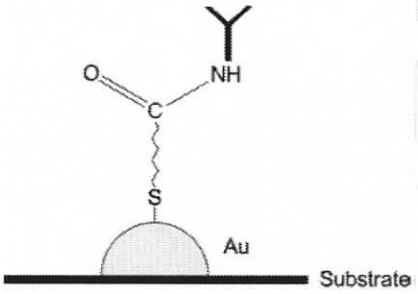

(c)

Figure 3.7 AFM image and analysis of IgG attached to gold nanoparticle arrays on glass substrate. (a): IgG nanoarrays. (b): Height analysis corresponding to (a) shows a height increase of ~7 nm compared to bare dots after protein attachment. (c): Schematic showing attachment of IgG.

Figure 3.8 shows a protein nanoarray derived from a colloidal mask using smaller (450 nm diameter) spheres, which demonstrates the versatility of the colloidal lithography approach in controlling the size and spacing of the dots in the nanoarray. The shape of the dots is also more circular due to the decreased size of the openings in the mask. Once again, attachment of antibodies was characterized via the increase in height of the gold dots. Previous literatures has shown that each IgG feature is 6.5±0.9 nm high when deposited on a gold thin-film surface [53, 84, 85]. Early literature demonstrates that a single IgG molecule has a height of 14.5 nm [53]. Therefore, it is believed that IgG molecules are not attached onto the gold surface in a perpendicular manner, but at an angle, perhaps due to the SAM molecules. Changes in protein conformation upon surface attachment and interaction with other proteins will also modify the observed height of IgG molecules.

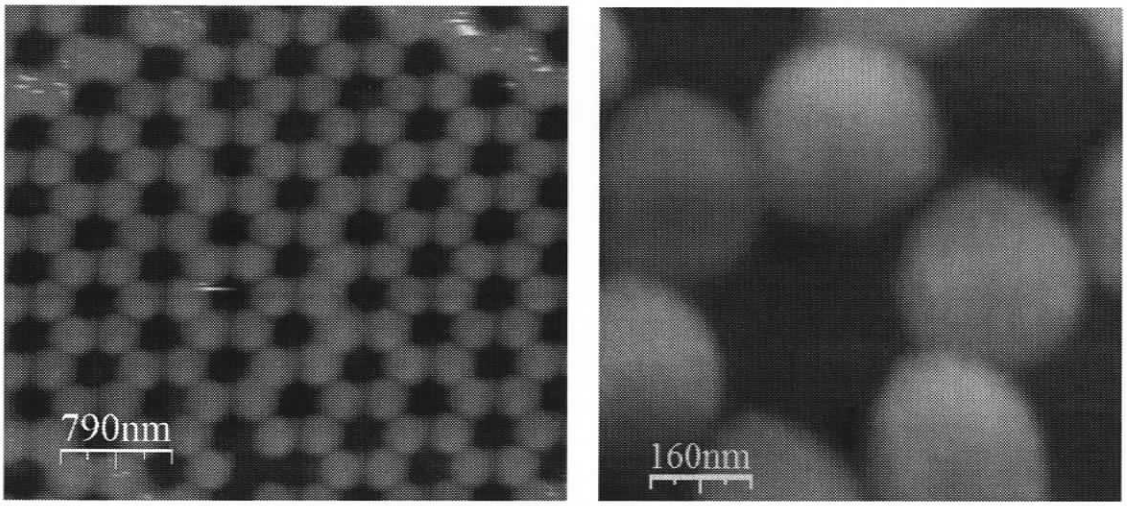

(a) **(b)**

Figure 3.8 AFM image of IgG attached gold nanoparticle array made with 450 nm colloidal spheres. (a) AFM image of an nanoarray after IgG attachment. (b) Close-up view showing protein molecules on gold dots. (Apparent width of dots is increased due to AFM tip convolution)

Figure 3.9 shows an AFM image of the glass substrate near gold and compared to the earlier samples (e.g., Figure 3.4), there are much fewer unwanted residues remaining on the glass substrate due to increased rinsing after each step.

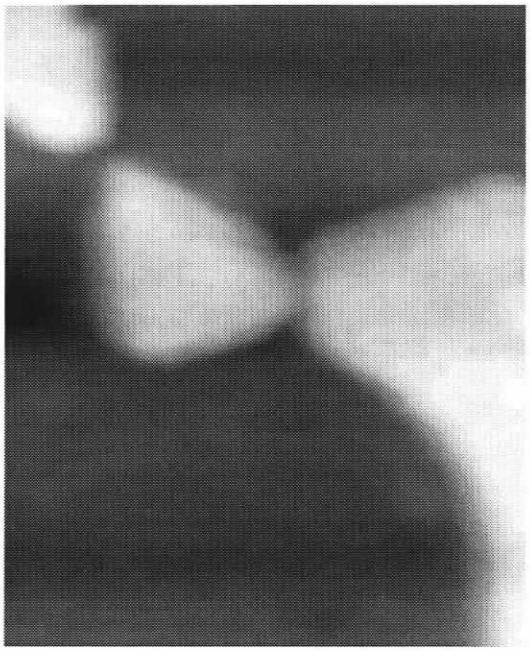

Figure 3.9 AFM image of reduced IgG attachment onto glass surface after improved rinsing of samples.

Silicon Substrate Samples

Figure 3.10 shows AFM images of a silicon substrate processed with polystyrene nanospheres have a diameter of 450 nm, and annealed at 105°C for 300 minutes. Before surface modification and protein attachment, the height of silicon region is ~40 nm. The height data in Figure 3.10 (b) shows that monolayer IgG molecules are attached on gold regions. Along with previous images obtained from different samples, this shows the

repeatability of our approach in attaching protein onto gold using colloidal lithography. Dot adhesion and non-specific binding was found to be most problematic on silicon thus far. Efforts to address these issues are ongoing due to the relevance of silicon in miniaturization of devices and sensors.

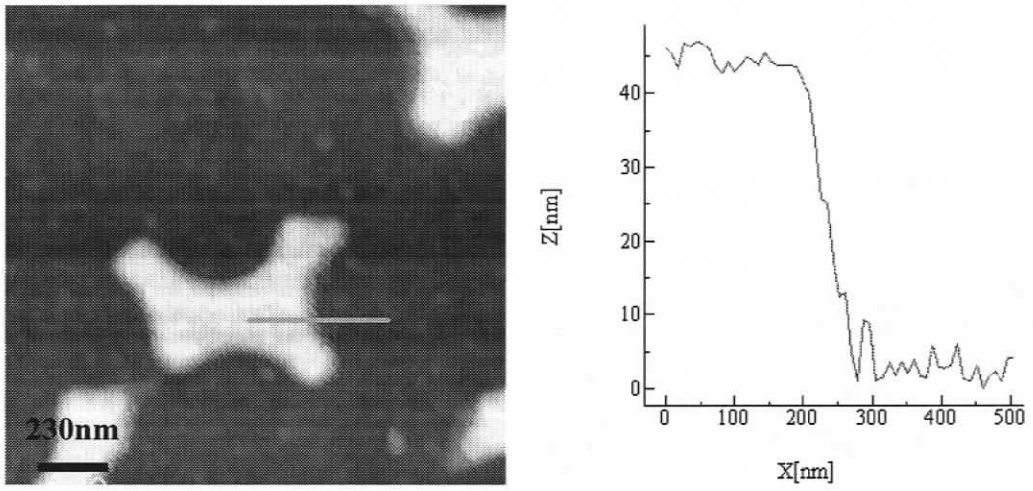

(a) (b)

Figure 3.10 AFM Image of Protein Attachment on Si Substrate. (a): AFM images show that IgG molecules are attached on gold region. (b): Height analysis shows that the height is ~45 nm after protein attachment.

3.1.4 Characterization of IgG-anti-IgG protein Arrays

To test the bioactivity of our IgG functionalized surfaces, we attempted to attach anti-IgG molecules. Figure 3.11 shows a gold strip region after anti-IgG attachment: The height increases to 57.5 nm. An increased height of about 7 nm indicates that a single monolayer of anti-IgG molecules is indeed attached to the IgG. Figure 3.11 (c) is a

schematic showing the attachment of anti-IgG in our structures. Similar experiments with better adhesion samples will be performed in the future.

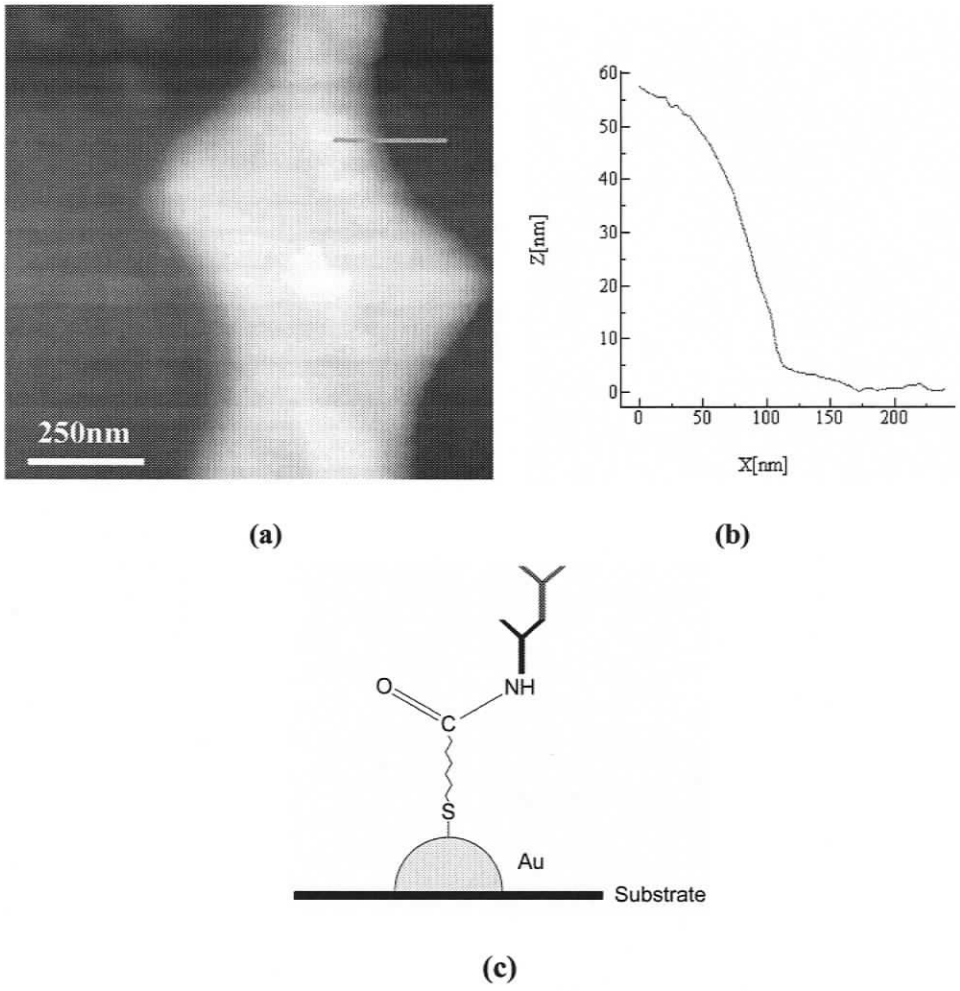

Figure 3.11 AFM image of anti-IgG Attachment. (a): Gold attached with IgG and anti-IgG molecules. (b): Height data show that the height goes up to ~58 nm after anti-IgG attachment. (c): A schematic of anti-IgG attachment to gold.

3.2 Characterization of Nanoarrays via SEM

3.2.1 Characterization of Gold Nanoparticle Arrays

Figure 3.12 shows SEM images of gold nanoparticle arrays on glass prior to functionalization. The mask was annealed under 105 ºC for 300 minutes, and the polystyrene nanospheres were 780 nm diameter. Hexagonal closed-packed nanoparticle arrays are formed on the substrate having a triangular shape.

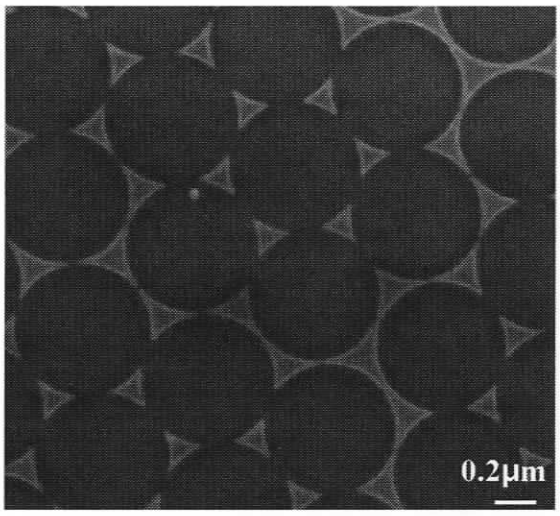

Figure 3.12 SEM images of gold nanoparticle arrays on glass substrate.

3.2.2 Characterization of IgG Protein Arrays

Figure 3.13 shows two SEM images of gold regions after protein attachment showing IgG molecules are attached onto gold. Most previous work used SEM to image larger biological structures, such as cells. These images indicate that although the protein

molecules are probably damaged during scanning, SEM is still a useful detection method to characterize proteins with nanoscale resolution.

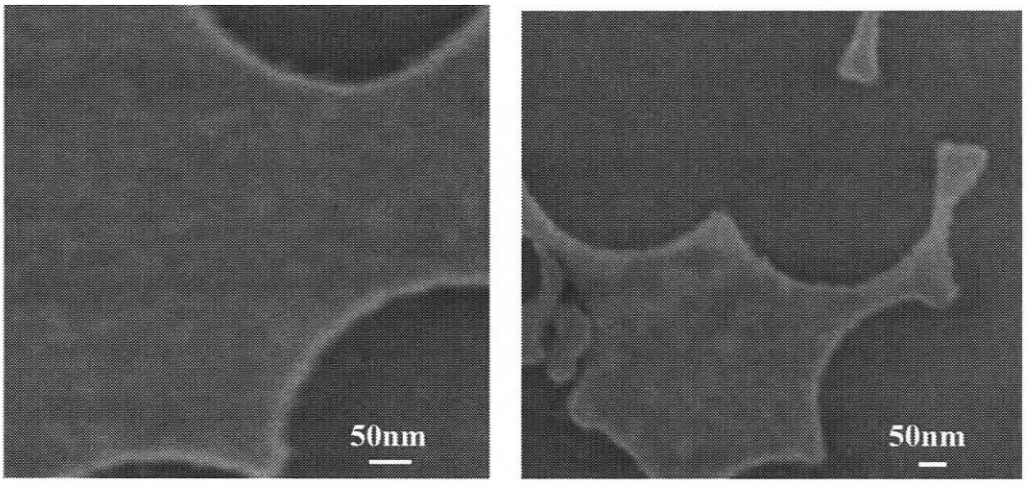

(a) (b)

Figure 3.13 SEM Images of IgG Attachment onto Gold Regions.

3.3 Discussion

In this chapter, we used AFM and SEM to characterize protein nanoarrays formed via colloidal lithography. Both AFM and SEM images show that we successfully formed gold nanoparticle arrays and attached proteins onto the nanoparticles through surface functionalization and target antibody attachment.

We addressed some problems in the process of fabricating the protein nanoarrays: The roughness of the gold nanoparticle surface was improved. A major challenge is keeping the gold dots on the surface during protein attachment. After we changed the conditions

of metal deposition, the adhesion of gold nanoparticles improved significantly on glass samples. However on silicon better adhesion is still required.

In addition, through AFM we were able to understand how rinsing after each sample processing step is important. We improved the rinsing methods after SAM formation and the NHS/EDC step, and non-specific binding was significantly reduced. In addition, after each step of protein attachment, rinsing several times with DI water helped get rid of non-specific binding of proteins onto glass and left single monolayer of proteins on gold nanoparticles.

Images of protein-attached gold nanoparticles from different samples indicate the viability of our protein nanoarray fabrication method. AFM analysis showed that a single monolayer of proteins is often attached. Also, via AFM we gained some insight into the orientation of protein molecules and the surface modification mechanism.

4 Conclusion

4.1 Summary of Thesis

In this thesis, we focused on the fabrication of protein nanoparticle arrays via colloidal lithography. In the first chapter, background on nanotechnology and nanoarrays was introduced. Biological and other applications of nanotechnology were briefly described. After an overview of nanotechnology, we introduced micro and nanoarrays. Advantages, current challenges, and applications of nanoarrays were described. This background provided us the motivation to fabricate protein nanoarrays using a simple and inexpensive colloidal patterning approach.

The general fabrication process involved formation of nanosphere monolayer masks; metal deposition; sphere removal; surface modification of nanoparticle arrays; and protein attachment. Before these steps, pre-treatment of the substrate was important to render the surface hydrophilic. Polystyrene nanospheres were used to create the masks for metal deposition. Metal nanoparticle arrays with a nanoparticle height of 40 nm and a diameter of 150 - 200 nm were obtained through metal deposition using an e-beam evaporator. Through surface modification of the nanoparticle arrays, proteins were covalently bound onto the metal nanoparticles. Different from previous work focusing on fabrication of protein nanoarrays via the colloidal approach, we used IgG antibodies in this work. After thorough rinsing, we successfully obtained monolayers of IgG protein

arrays with a height increase of approximately 6-7 nm, and attached anti-IgG molecules with a similar height increase to demonstrate the bioactivity of our IgG modified surfaces.

We characterized our samples using AFM and SEM. These nanoscale characterization methods helped us understand each fabrication step at a molecular level and provided promising avenues for further research.

Multiplexed detection of many proteins can be achieved by multiple spotting methods. For large-scale fabrication, although we only have a relatively small total area in this work for our proof-of-concept, the method we used is a large area approach. Also, the fabrication cost of our method is much less than $100 CDN per sample, which is relatively low compared to most nanopatterning methods.

4.2 Future Work

Our work provides a potential tool for both scientific research and clinical disease diagnostics. The nanoscale protein nanoarrays can be used to detect interactions between proteins, proteins and other biomolecules, and also proteins and cells. In addition, in drug discovery research, it can be used to discover new drugs and test the bioactivity of new drugs. Clinically, the nanoscale protein arrays can be applied to detect diseases at an early stage, for example, to detect cancer at a very early stage via various biomolecular marker assays. Only a very small amount sample is required, and the cost is low.

Although the protein nanoarrays demonstrated in this work provide a promising tool for biomedicine, there are still challenges that need to be addressed. As mentioned in the first chapter, non-specific binding is a main issue for nanoscale protein arrays. Although we tried to do a thorough rinse after each protein attachment step, there are still some residues left on background sites. Future work can use different methods, such as polyethylene glycol (PEG) attachment onto the substrates to prevent or block non-specific binding interactions. Also, other solutions, such as Tween-20 can be used to rinse the samples after protein attachment.

Another major issue of our work is that the adhesion of nanoparticles needs to be improved. As shown in the third chapter, often gold dots were removed after surface functionalization and protein attachment, particularly on silicon.

Although colloidal lithography has some advantages over conventional lithography, there are still some problems to be solved, such as defect formation during self-assembly [57]. So far with the development of colloidal patterning methods some approaches to remove the defects in colloidal arrays have been explored, and it is promising that colloid arrays with no or tolerable defects over large areas could be achieved in the future [57].

For the fabrication of nanosphere masks, contact angle measurements can be used to measure the degree to which a surface has been made hydrophilic prior to depositing the colloidal dispersion [88].

In the future, other detection methods can be applied to help detect protein attachment and understand the interactions at a molecular level. For example, localized surface plasmon resonance and Raman spectroscopy have been used to characterize nanoscale arrays, and could be employed with our structures as well. Also, for future sensor design, different types of output signals can be produced for detection, such as optical signals and electrical signals by integrating our protein nanoarrays with other methods. For example, the arrays might be integrated into an electrochemical electrode sensor. The proteins of interest in solution are oxidized by enzymes and further reduced electrochemically by the electrode under a working potential [89]. Figure 4.1 shows a schematic of a biosensor based on our protein nanoarrays. For these applications, and more generally, fabricating protein nanoarrays with various diameter particles will be important. The colloidal approach we employed here is ideally suited to this type of tunability.

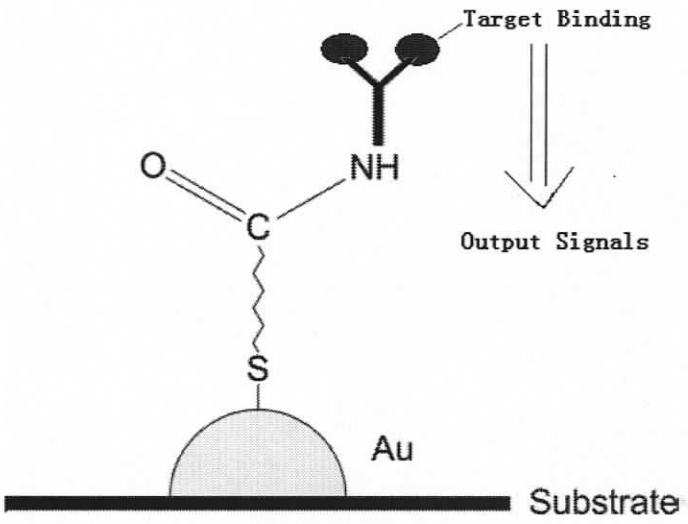

Figure 4.1 A schematic of a biosensor based on our protein nanoarrays. Primary proteins are attached onto gold nanoparticle arrays. Output signals are produced when target binding of interested biomarkers happens. The schematic is not drawn to scale.

The IgG and anti-IgG we used are typical model molecules in immunological research. Future work could employ disease biomarkers, such as Prostate Specific Antigen (PSA) and anti-PSA molecules to test the bioactivity of the nanoarrays. High-density arrays can potentially detect these biomarkers more accurately. Further, with improved control of the fabrication process and little non-specific binding interactions, our protein nanoarrays may be used in real blood tests and ultimately help improve the quality of life.

Bibliography

[1] http://www.nano.gov/html/facts/whatIsNano.html

[2] http://www.zyvex.com/nanotech/feynman.html

[3] Norio Taniguchi. Japan Society of Precision Engineering, 1974.

[4] S. Salapaka, M. Salapaka, IEEE Control Systems Magazine, volume 28, p 65-83, 2008.

[5] C. Peterson. IEEE Computer, volume 33, p 46-53, 2000.

[6] M. C. Roco, Journal of Nanoparticle Research, volume 7, p 707-712, 2005.

[7] C. Papadopoulos, ELEC 420 Nanotechnology Lecture Notes, Spring 2007, University of Victoria, Canada.

[8] Cao G. *Nanostructures and Nanomaterials: Synthesis, Properties and Applications.* Imperial College Press, 2004.

[9] H. Gronbeck, J. Thomas, Chemical Physics Letters, volume 443, p 337-341, 2007.

[10] G. Chai, Y. Sun, J. Sun, Q. Chen, Journal of Micromechanics and Microengineering, volume 18, p 035013, 2008.

[11] D. Li, Y. Wu, P. Kim, S. Li, P. Yang, A. Majumdar, Applied Physics Letters, volume 83, p 2934-2936, 2003.

[12] R. M. Costescu, D.Cahill, F. Fabrequette, Z. Sechrist, S. George, Science, volume 303, p 989-990, 2004.

[13] M. A. Panzer, G. Zhang, D. Mann, X. Hu, E. Pop, H. Dai, K. Goodson, Journal of Heat Transfer, Volume 130, p 052401-1-9, 2008.

[14] G. Maracas, D. Johnson, R. Puechner, J. Edwards, S. Myhajlenko, H. Goronkin, R. Tsui, Solid-State Electronics, volume 32, p 1887-1893, 1989.

[15] E. Gombia, R. Mosca, S. Franchi, P. Frigeri, C. Ghezzi, Materials Science and Engineering C, volume 26, p 867-870, 2006.

[16] H H Yao, Y. Wang, M. Qu, H. Kuo, S. Wang, C. Lin, Nanotechnology, volume 17, p 664-667, 2006.

[17] X. Sun. Molecular Physics, volume 100, p 3059-3063, 2002.

[18] S. M. Moghimi, Pharmacological Reviews, volume 53, p 283-318, 2001.

[19] http://nano.cancer.gov/about_alliance/cancer_nanotechnology_plan.asp

[20] J. Hoh, J. Revel, P. Hansma, The International Society for Optical Engineering, volume 1639, p 212-215, 1992.

[21] S. Hell. Nature Biotechnology, volume 21, p 1347-1355, 2003.

[22] R. Narayanaswamy, Optical Sensors. Asian Conference on Sensors and the International Conference on New Techniques in Pharmaceutical and Biomedical Research-Proceedings, 2005.

[23] D. Kim. Journal of the Optical Society of America, volume 23, p 2307-2314, 2006.

[24] E. Carlen, A. Van den Berg, Lab on a Chip, volume 7, p 19-23, 2007.

[25] W. Ruan, P. Eastman, P. Cooke, J. Park, J. Chu, J. Gray, S. Li, F. Chen, Advances in Space Research, volume 40, p 513-522, 2007.

[26] J. M. Perez, J. Lee, T. O'Loughlin, D. Hogemann, R. Weissieder, Nature Biotechnology, volume 20, p 816-820, 2002.

[27] D. C. Drummond, Pharmacological Reviews, volume 51; p 691-743, 1999.

[28] J. L. Au, Journal of Control Release, volume 74; p 31-46, 2001.

[29] G. J. Fetterly, AAPS Pharmaceutical Science, volume 5, p 1843-1854, 2003.

[30] O. M. Koo, I. Rubinstein, H. Onyuksel, Nanomedicine: Nanotechnology, Biology, and Medicine, volume 1, p 193-212, 2005.

[31] O. Koo, I. Rubinstein, H. Onyuksel, Nanomedicine, volume 1, p 77-84, 2005.

[32] A. Arnedo, J. Irache, M. Merodio, M. Espuelas, Journal of Control Release, volulme 94, p 217-227, 2004.

[33] D. Surneet, Journal of Controlled Release, volume 93, p 123-133, 2003.

[34] T. Yih, C. Wei, Nanomedicine: Nanotechnology, Biology, and Medicine, volume 1, p 191-192, 2005.

[35] R. Bakalova, H. Ohba, Z. Zhelev, T. Nagase, R. Jose, M. Ishikawa, Y. Baba, Nano Letters, volume 4, p 1567-1573, 2004.

[36] K. Prashant, Nanotoday, volume 2, p 18-29, 2007.

[37] K. Crowder, M. Hughes, J. Marsh, A. Barbieri, R. Fuhrhop, G. Lanza, S. Wickline, Ultrasound in Medicine and Biology, volume 31, p 1693-1700, 2005.

[38] L. Miranda, Biopolymers, volume 55, p 217-226, 2000.

[39] A. Lueking, M. Horn, H. Eickoff, K. Bussow, H. Lehrach, G. Walter, Analytical Biochemisty, volume 270, p 103-111, 1999.

[40] B. Van Weemen, FEBS Letters, volume 18, p 232-236, 1971.

[41] L. G. Mendoza, P. McQuary, A. Mongan, R. Gangadharan, S. Brignac, M. Eggers, Biotechniques, volume 27, p 778-785, 1999.

[42] R. M. de Wildt, C. Mundy, B. Gorick, I. Tomlinson, Nature Biotechnology, volume 18, p 989-994, 2000.

[43] G. MacBeath, S. Schreiber, Science, volume 289, p 1760-1763, 2000.

[44] D. R. Cox, Proceedings of the Annual International Conference on Computational Molecular Biology, p 60, 1998.

[45] http://www.hupo.org/

[46] J. Glokler, P. Angenendt, Journal of Chromatography B Analytical Technologies in the Biomedical and Life Sciences, volume 797, p 229-240, 2003.

[47] C. Situma, M. Hashimoto, S. Soper, Biomolecular Engineering, volume 23, p 213-231, 2006.

[48] G. Moore, Proceedings of SPIE, volume 2438, p 2-17, 1995.

[49] M. Lynch, NSTI Nanotechnology Conference and Trade Show, p 35-38, 2004.

[50] Y. Cai, B. Ocko, Langmuir, volume 21, p 9274-9279, 2005.

[51] J. Li, Sensors and Actuators B (Chemical), volume 110 , p 378-382, 2005.

[52] N. Kumar, P. Omkar, H. Jong-in, Journal of Physical Chemistry B, volume 111, p 4581-4587, 2007

[53] C. Wingren, Drug Discovery Today, volume 12, p 813-819, 2006.

[54] K. Lee, S. Park, C. Mirkin, J. Smith, M. Mrksich, Science, volume 295, p 1702-1705, 2002.

[55] L. Lyklema. *Fundamentals of Interface and Colloid Science*, volume 2, p 3208, 2005.

[56] Y. A. Vlasov, X. Bo, J. Sturm, D.J. Norris, Nature, volume 414, p 289-293, 2001.

[57] S. Yang, S. Jang, D. Choi, S. Kim, H. Yu, Small, volume 2, p 458-475, 2006.

[58] J. Jeong, S. Kim, S. Kim, J. Bland, S. Shin, S. Yang, Small, volume 3, p 1529-1533, 2007.

[59] E. Hutter, J. Fendler, Advanced Materials, volume 16, p 1685-1706, 2004.

[60] W. Li, Applied Surface Science, volume 253, p 9035-9038, 2007.

[61] B. Tan, C. Sow, T. Koh, K. Chin, A. Wee, C. Ong, Journal of Physical Chemistry, volume 109, p 11100-11109, 2005.

[62] A. Kosiorek, W. Kandulski, H. Glaczynska, M. Giersig, Small, volume 1, p 439-444, 2005.

[63] R. Lenigk, M. Carles, N. Ip, N. Sucher, Langmuir, volume 17, p 2497-2501, 2001.

[64] O. D. Velev, T. Jede, R. Lobo, A. Lenhoff, Nature, volume 389, p 447, 1997.

[65] P. Jiang, Chemistry of Materials, volume 11, p 519-521, 1999.

[66] F. Jarai-Szabo, S. Astilean, Z. Neda, Chemical Physics Letters, volume 408, p 241-246, 2005.

[67] S. Winnitoy. Nanosphere Lithography Substrate Preparation Notes, University of Victoria, 2007.

[68] C. Papadopoulos, R. S. van den Boogaard, S. Clutterbuck, G. M. Lindsay, S. R. Winnitoy, Nanotechnology, volume 18, p 245306-245310, 2007.

[69] C. Lee, Applied Optics, volume 44, p 7333-7338, 2005.

[70] A. Kohut, A. Voronov, W. Peukert, Particle and Particle Systems Characterization, volume 22, p 329-335, 2006.

[71] A. Marie-Eve, K. Hamad-Schifferli, Langmuir, volume 21, p 12080-12084, 2005.

[72] M. Veiseh, M. Zareie, M. Zhang, Langmuir, volume 18, p 6671-6678, 2002

[73] D. J. Revell, J. Knight, D. Blyth, A. Haines, D. Russell, Langmuir, volume 14, p 4517-4524, 1998.

[74] S. Ferretti, Trends in Analytical Chemistry, volume 19, p 530-540, 2000.

[75] A. Ulman, *An Introduction to Ultrathin Organic Films*, Academic Press, Boston, MA, 1991.

[76] A. Ulman, Chemical Reviews, volume 96, p 1533-1554, 1996.

[77] C. D. Bain, Journal of American Chemical Society, volume 111, p 321, 1989.

[78] M. Wissink, R. Beernink, J. Pieper, A. Poot, G. Engbers, T. Beugeling, W. van Aken, J. Feijen, Biomaterials, volume 22, p 151-163, 2001.

[79] O. Ouerghi, A. Touhami, A. Othrnane, H. Ben Ouada, C. Matelet, C. Fretigny, N. Jaffrezic-Renault, Sensors and Actuators B, volume 84, p 167-175, 2002.

[80] Junqueira, Luiz C.; Jose Carneiro, *Basic Histology*. McGraw-Hill, 2003.

[81] ghr.nlm.nih.gov/handbook/illustrations/igg

[82] J. Lee, S. Sim, S. Cho, J. Lee, Biosensors and Bioelectronics, volume 20, p 1422-1427, 2005.

[83] Z. Wang, Y. Yang, J. Li, J. Gong, G. Shen, R. Yu, Talanta, volume 69, p 686-690, 2006.

[84] T. Hugli, *Techniques in protein chemistry*, Academic Press, San Diego, 1989.

[85] H. Zhang, K. Lee, Z. Li, C. Mirkin, Nanotechnology, volume 14, p 1113-1117, 2003.

[86] M. E. Browning-Kelley, K. Wadu-Mesthrige, V.Hari, G. Liu, Langmuir, volume 13, p 343-350, 1997.

[87] J. R. Kenseth, J. Harnisch, V. Jones, M. Porter, Langmuir, volume 17, p 4105-4112, 2001.

[88] O. N. Tretinnikov, Langmuir, volume 16, p 2751-2755, 2000.

[89] M. Chuang, C. Liu, M. Yang, Sensors and Actuators B, volume 114, p 357-363, 2006.